MECHANICAL AND HYDRAULIC PERFORMANCE OF

CEMENT GROUTS FROM 5 SUPPLIERS IN THAILAND

Wuttichai Samaiklang

A Thesis Submitted in Partial Fulfillment of the Requirements for the

Degree of Master of Engineering in Geotechonolgy

Suranaree University of Technology

Academic Year 2012

ประสิทธิภาพเชิงกลศาสตร์และชลศาสตร์ของซีเมนต์ยาแนว
จาก 5 ผู้จำหน่ายในประเทศไทย

นายวุฒิชัย สมัยกลาง

วิทยานิพนธ์นี้เป็นส่วนหนึ่งของการศึกษาตามหลักสูตรปริญญาวิศวกรรมศาสตรมหาบัณฑิต
สาขาวิชาเทคโนโลยีธรณี
มหาวิทยาลัยเทคโนโลยีสุรนารี
ปีการศึกษา 2555

MECHANICAL AND HYDRAULIC PERFORMANCE OF
CEMENT GROUTS FROM 5 SUPPLIERS IN THAILAND

Suranaree University of Technology has approved this thesis submitted in partial fulfillment of the requirements for a Master's Degree.

Thesis Examining Committee

_____

(Assoc. Prof. Kriangkrai Trisarn)

Chairperson

_____

(Assoc. Prof. Dr. Kittitep Fuenkajorn)

Member (Thesis Advisor)

_____

(Dr. Decho Phueakphum)

Member

_____   _____

(Prof. Dr. Sukit Limpijumnong)   (Assoc. Prof. Flt. Lt. Dr. Kontorn Chamniprasart)

Vice Rector for Academic Affairs   Dean of Institute of Engineering

วุฒิชัย สมัยกลาง : ประสิทธิภาพเชิงกลศาสตร์และชลศาสตร์ของซีเมนต์ยาแนว
จาก 5 ผู้จำหน่ายในประเทศไทย (MECHANICAL AND HYDRAULIC
PERFORMANCE OF CEMENT GROUTS FROM 5 SUPPLIERS IN THAILAND)
อาจารย์ที่ปรึกษา : รองศาสตราจารย์ ดร.กิตติเทพ เฟื่องขจร, 95 หน้า.

วัตถุประสงค์ของการศึกษานี้เพื่อประเมินประสิทธิภาพเชิงกลศาสตร์และชลศาสตร์ของ
ซีเมนต์ยาแนวเกรดการค้าในรอยแตกของหิน ค่าที่ได้ถูกเปรียบเทียบในเทอมของ กำลังกด
สัมประสิทธิ์ความยืดหยุ่น ความซึมผ่าน และกำลังเฉือนสำหรับการยาแนวรอยแตกของหิน โดยทำ
การทดสอบปูนซีเมนต์ปอร์ตแลนด์ประเภทที่ 1 ตามมาตรฐาน ASTM C150 จาก 5 บริษัทผู้ผลิตและ
จำหน่ายซีเมนต์ชั้นนำของประเทศไทย ผลการวิจัยพบว่า ค่าความหนืดของซีเมนต์เหลวอยู่ระหว่าง
0.6 – 0.8 ปาสคาล·วินาที ค่ากำลังกดของซีเมนต์หลังจากการบ่ม 28 วันคือ 25.77±2.54 เมกะ
ปาสคาล ค่ากำลังกดของซีเมนต์ที่สูงที่สุดคือปูนซีเมนต์จากบริษัทปูนซีเมนต์ไทย มีค่าเท่ากับ
27.64±2.67 เมกะปาสคาล ค่ากำลังดึงที่สูงที่สุดคือปูนซีเมนต์จากบริษัทเซเม็กซ์ไทยแลนด์ มีค่า
เท่ากับ 2.95±0.10 เมกะปาสคาล กำลังยึดติดของซีเมนต์มีค่าเท่ากับ 1.90±0.42 โดยปูนซีเมนต์ที่ให้
กำลังยึดติดสูงที่สุดคือปูนซีเมนต์จากบริษัทปูนซีเมนต์นครหลวง การตรวจวัดความซึมผ่านของ
ซีเมนต์ยาแนวพบว่าเมื่อระยะเวลาการบ่มเพิ่มขึ้นสัมประสิทธิ์การซึมผ่านของซีเมนต์จะลดลง ความ
เหมือนและแตกต่างกันของประสิทธิภาพการยาแนวในเชิงคุณสมบัติทางด้านกลศาสตร์และชล
ศาสตร์ ของซีเมนต์ยาแนวเกรดการค้า ได้ถูกเปรียบเทียบเพื่อการประยุกต์ใช้ซีเมนต์ยาแนวในรอย
แตกของหิน

สาขาวิชา เทคโนโลยีธรณี   ลายมือชื่อนักศึกษา _____
ปีการศึกษา 2555   ลายมือชื่ออาจารย์ที่ปรึกษา _____

WUTTICHAI SAMAIKLANG : MECHANICAL AND HYDRAULIC PERFORMANCE OF CEMENT GROUTS FROM 5 SUPPLIERS IN THAILAND. THESIS ADVISOR : ASSOC. PROF. KITTITEP FUENKAJORN, Ph.D., PE., 95 PP.

ROCK FRACTURE/BOND STRENGTH/PORTLAND CEMENT/PERMEABILITY /GROUTING

The objective of this study is to assess the mechanical and hydraulic performance of commercial grade cement grouts in rock fracture. Their results are compared in terms of compressive strength, elastic modulus, permeability and shear strength for against rock fracture. The ordinary Portland cement (ASTM C150) type 1 from five cement supplier in Thailand have been tested. The results indicate that the viscosity of grout slurry it is 0.6 - 0.8 Pascal·sec. The compressive strength after 28 day curing times is 25.77 ± 2.54 MPa. The highest compressive strengths is from SCG cement supplier equal to 27.64 ± 2.67 MPa. The average tensile strength is 2.80 ± 0.27 MPa. The highest tensile strength is from CEMEX Thailand equal to 2.95 ± 0.10 MPa. The bond strength is 1.90 ± 0.42 MPa. The highest bond strength is from SCCC. When the curing time increases the intrinsic permeability of cement grouts decreases. Similarities and discrepancies of the grouting performance in terms of mechanical and hydraulic properties are compared to apply the commercial grade cement grouts in rock fractures.

School of ___Geotechnology___   Student's Signature_____

Academic Year 2012   Advisor's Signature _____

ACKNOWLEDGEMENTS

Wuttichai Samaiklang

TABLE OF CONTENTS

Page

TABLE OF CONTENTS (Continued)

LIST OF TABLES

LIST OF FIGURES

Figure   **Page**

LIST OF FIGURES (Continued)

LIST OF FIGURES (Continued)

LIST OF FIGURES (Continued)

SYMBOLS AND ABBREVIATIONS

c	=	Cohesion
i	=	Hydraulic gradient
ϕ	=	Internal friction angle
γ	=	Unit weight of water
μ	=	Dynamic viscosity
σ_1	=	Maximum principal stress
σ_3	=	Minimum principal stress
σ_B	=	Brazilian tensile strength
σ_c	=	Uniaxial compressive strength
σ_n	=	Normal stress
τ	=	Shear stress
ξ	=	Empirical constant

CHAPTER I

INTRODUCTION

1.1   Background of problems and significance of the study

Grouting is a procedure that involves grout injection into voids, fractures, and cavities in rock mass in order to improve their strength and durability, to reduce permeability, or to reduce the deformability of the rock formations. The ordinary Portland cement (OPC) in the forms of cement-water, cement-water-sand, cement-water-additive, or cement-water-sand-additive combinations is usually used. Characteristics of the grouts are influenced by many variables. The important ones include water-cement ratio (W/C), chemical compositions, fineness of the cement, additives to the grout, speed of mixing, mixing time, efficiency of mixing, and temperature (Anagnostopoulos, 2006).

This study does not attempt to evaluate these variables; rather, it is aimed at measuring relative shear strengths between cement grout and rock fracture, grout fluidity and their strength and elastic after curing. The cements slurry has been tested to determine the viscosity, density and flowability properties. The uniaxial compressive strength, Brazilian tensile strength, triaxial compressive strength, and the elastic modulus of the cured grouts are determined. Cylinders of the Phu Kradung sandstone are casted with the grouts for the four point bending and push out tests to determine the bond strength between the grout and rock fracture.

1.2   Research objectives

The objective of this study is to assess the mechanical and hydraulic performance of the commercial grade cement grouts in rock fracture. Their results are compared in terms of compressive strength, elastic modulus, permeability and bond strength against rock fracture, and to identify the viscosity, density and flowability properties of the grouts slurry. Five types of the commercial grade cement grouts have been studied.

1.3   Research methodology

As shown in Figure 1.1, the research methodology comprises 9 steps; literature review, sample collection and preparation, flowability test of grout slurry, basic mechanical properties test of cement grouts, bond strength testing , permeability of grouting material, data analysis and comparison, discussions and conclusions, and thesis writing and presentation.

1.3.1   Literature review

Literature review was carried out to study the experimental researches on the cement grout, and grouting materials. The sources of information are from text books, journals, technical reports and conference papers. A summary of the literature review are given in this thesis.

1.3.2   Sample collection and preparation

The grouting materials in this study are ordinary Portland cement ASTM (C150) type 1 obtained from five cement suppliers in Thailand. The fractures in rock cylinders are artificial made by line loading in Phu Kradung sandstone blocks. This fine-grained rock has highly uniform texture and widely exposes in the north and

northeast of Thailand. The grout preparation follows the ASTM (C938) standard practice using a Hobart type laboratory mixer. All grouts are prepared by mixing at the water-to-cement ratio of 0.60. The sample preparation was carried out in the Geomechanics Research (GMR) Laboratory at Suranaree University of Technology.

1.3.3 Flowability test of grout slurry

The flowability tests include rheological and density tests of freshly mixed cement grouts. The rheological test measures the viscosity and the shear stress used the viscometer follows the ASTM (D2196) standard practice. The density test follows the ASTM (D854) standard practice.

1.3.4 Basic mechanical properties test of cement grout

The basic mechanical properties tests include uniaxial triaxial compressive strength and Brazilian tension test. The cement slurry mixtures are poured and cured in 54 mm diameter PVC pipe. The specimens are cured under distilled water at room temperature (ASTM C192) before testing.

The uniaxial compressive strength tests are to determine strength and elastic modulus of cylindrical grouting specimens. The test procedure follows the ASTM (C39) and the ISRM suggested methods. The compressive strength of the grouts are measured from cylindrical specimens with a diameter of 54 mm and L/D = 2.5 in cylinder that is cured in PVC pipe. Strength measurements are made at 3, 7, 14, and 28 days curing.

The Brazilian tension test determined the indirect tensile strength of the cement grouts. The test procedure follows the ASTM (D3967) and the ISRM suggested methods. One hundreds samples with a diameter of 54 mm are tested with L/D = 0.5. Strength measurements are made at 3, 7, 14, and 28 days curing.

The triaxial compressive strength tests determine the triaxial compressive strength, elastic modulus, and Poisson's ratio of the cured grouts. The test procedure follows the ASTM (D7012) standard practice. The cement grouts with a diameter of 54 mm are tested with L/D = 2.0. The test employs a high-pressure, high-capacity triaxial cell (Hoek Cell). The specimen is enclosed in a rubber membrane and sealed with the loading cap. Strength measurements are made after 28 days curing.

1.3.5 Bond strength testing

Two bond strength test methods are used to determine the adhesive ability of the cement grouts. They are the four point bending test and the push out test.

The four point bending test determined the bond strength of cement grout and rock fracture. The test procedure follows the ASTM (D6272). The cement grout is casted on the rough end of the rock cylinder with a diameter of 54 mm and length of 200 mm. Five cement grouts are investigated after 28 days curing.

Push out test determined the push out strength of cement grout casted in a hole at the center of the specimen with a diameter of 35 mm and length of 70 mm. The cement grouts casted in the hole at the center of Phu Kradung sandstone are investigated after 28 days curing.

1.3.6 Permeability of grouting materials

The permeability of grouting materials is determined in terms of the intrinsic permeability (k). The constant head flow test is conducted to measure the longitudinal permeability of the grout. The cylinder specimen is 10 cm in diameter and 10 cm long. After three days of curing, the specimen is carefully removed from

the cast (PVC pipe), cleaned, and placed in water bath before installing in the permeability test apparatus. The permeability of the test system is measured and recorded at 3, 7, 14, and 28 days of curing periods.

```
                    ┌──────────────────────┐
                    │ 1. Literature review │
                    └──────────┬───────────┘
                               │
                    ┌──────────▼───────────┐
                    │ 2. Sample collection │
                    │    and preparation   │
                    └──────────┬───────────┘
                               │
   ┌──────────┐     ┌──────────▼───────────┐     ┌──────────┐
   │  Slurry  │────▶│ 3. Flowability test  │     │  Grouts  │
   └──────────┘     │    of grout slurry   │     └──────────┘
                    └──────────────────────┘
```
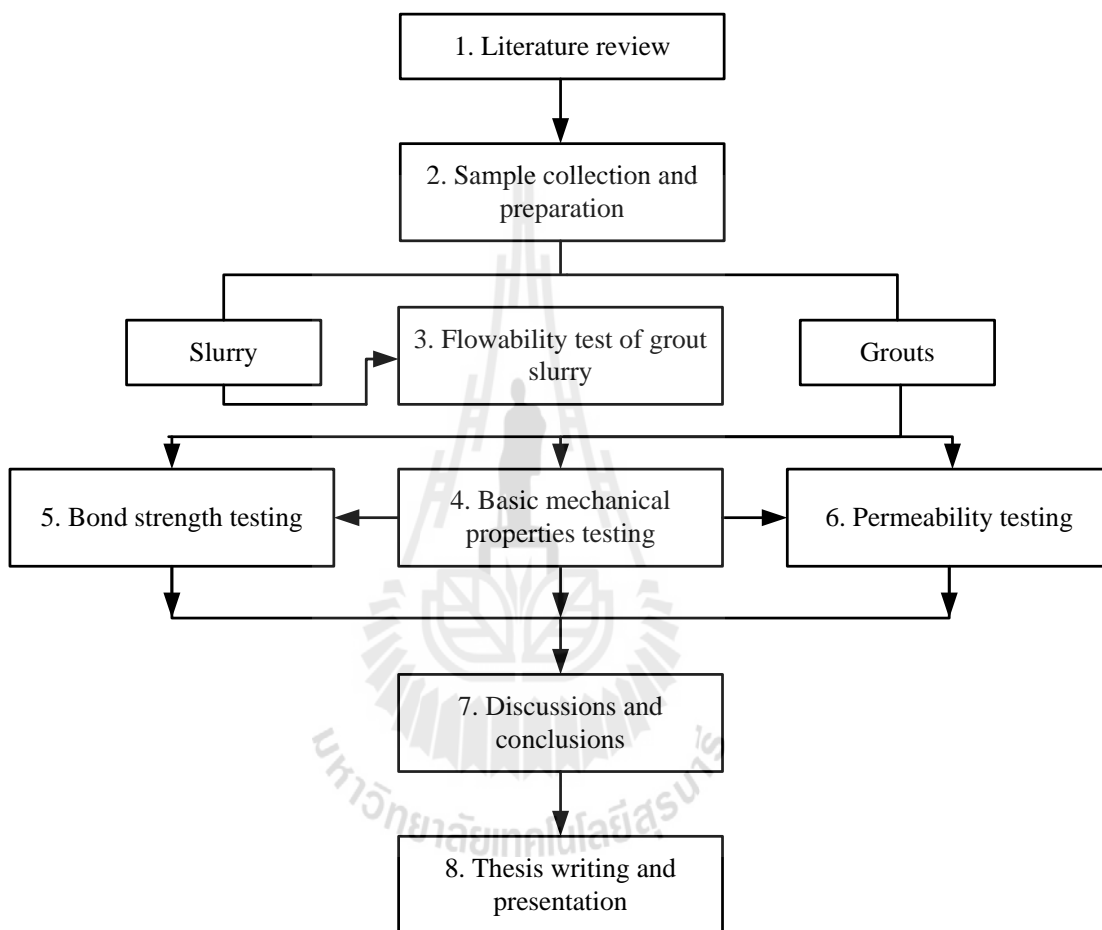
Figure 1.1 Research methodology

1.3.7 Discussions and conclusions

Discussions of the results are described to determine the reliability and accuracy of the measurements. Performance of the commercial grade cements grouts are discussed based on the test results. Similarities and discrepancies of the grouting materials in terms of the mechanical and hydraulic properties are discussed to apply the commercial grade cement grouts for grouting in rock fractures. The research results are concluded.

1.3.8 Thesis writing and presentation

All research activities, methods, and results was documented and complied in the thesis. The research or findings will be published in the conference proceedings or journals.

1.4 Scope and limitations of the study

The scope and limitation of the research include as follows.

1. The commercial grade cement grouts in this study are ordinary Portland cement ASTM (C150) type 1 obtained from five cement suppliers in Thailand, including

    1.1 Asia Cement Public Company Limited (ACC).

    1.2 CEMEX Thailand Cement Public Company Limited (CEMEX).

    1.3 Siam Cement Group Public Company Limited (SCG).

    1.4 Siam City Cement Public Company Limited (SCCC).

    1.5 TPI Polene Cement Public Company Limited (TPI).

2. The laboratory tests include uniaxial-triaxial compressive strength, Brazilian tensile strength, four point bending and push out tests between

rock fracture and grouting materials and flowability properties testing of grout slurry.

3. Laboratory testing was conducted on Phu Kradung sandstone specimens only.

4. All tested fractures used artificially made in the laboratory by tension induced method.

5. All tests are conducted under ambient temperature.

6. No field testing is conduct.

1.5   Thesis contents

Chapter I introduces the thesis by briefly describing the background of problems and significance of the study. The research objectives, methodology, scope and limitations are identified. **Chapter II** summarizes results of the literature review. **Chapter III** describes the sample preparation. **Chapter IV** presents the laboratory experiment and results obtained from the grout slurry testing. **Chapter V** presents the mechanical and hydraulic properties experiment and results obtained from the laboratory testing.   **Chapter VI** concludes the research results, and provides recommendations for future research studies.

CHAPTER II

LITERATURE REVIEW

2.1   Introduction

Grouting is a special technique developed in recent years with many applications. It is a procedure that involves grout injection into voids, fissures, and cavities in soil or rock formation in order to improve their properties, specifically to reduce permeability, to increase strength and durability or to lessen deformability of the formations. Grouting has a wide application in the modern civil engineering world (Nonveiller 1989, Fransson 2001, Yesilnacar 2003, Yeon and Han 1997). Various materials are used for grouting depending on the purpose of the grouting and the properties of the grouted rock or soil (Anagnostopoulos and Hadjispyrou 2004). The conventional method currently used to improve the mechanical properties of rock mass is the grouting with ordinary Portland cement (OPC). The ordinary Portland cement (OPC) in the forms of cement-water, cement-water-sand, cement-water-additive, or cement-water-sand-additive combinations is usually used. Characteristics of the grouts are influenced by many variables. The important ones include water-cement ratio (W/C), chemical compositions, fineness of the cement, additives to the grout, speed of mixing, mixing time, efficiency of mixing, and temperature (Anagnostopoulos, 2006). This chapter summarizes the results of literature review carried out to improve an understanding of the application for grouting material in rock fracture. The topics reviewed here include (1) flowability of slurry, (2) strength

of cured grout, (3) permeability of the grout, and (4) experimental researches on cement and rock fracture (bond strength, shear strength, and push out test).

2.2 Literature review

2.2.1 Flowability of slurry

Frantzis and Baggott (1997) rheological characteristics of rapid setting magnesia phosphate-based slurries determined with a rotating viscometer incorporating an interrupted helical impeller are reported. The investigations also included an evaluation of the effect of test specimen dimensions and comparisons with an ordinary Portland cement based reference slurry. The test procedure adopted comprised measuring the stress response to three repetitive speed cycles undertaken over a 15 minutes period immediately after slurry preparation. The results are assessed in the practical context of the use of retarded slurry to infiltrate a steel fiber reinforcing array. An empirical treatment of the data is presented which provides the basis for assessing the influence of viscosity during vibratory infiltration as well as providing some insight into hysteresis phenomena and test procedure.

Mesbah and Yahia (1998) the ability to assess rheological properties of neat cement grout, such as those used in structural repair and for filling post tension ducts, is of special interest for the evaluation of the ease of pumping, spreading into place, and filling of narrow spaces. There is an increasing need to identify dependable and simple test methods that can characterize the consistency of specialty cement grouts and reflect variations in rheological properties during handling and placement. Several tests can be used to evaluate the rheological characteristics of a cement grout

suspension, including precise methods for the determination of rheological parameters and simple procedures to assess fluidity. Rheological properties can be accurately determined by using a coaxial cylinder viscometer. However, the use of such a viscometer is mainly limited to the laboratory, and simple methods including the mini slump spread and the modified Marsh cone tests are usually employed in the field to verify the consistency for quality control.

The flow behavior of grout materials is governed by their rheological properties. Various devices are used for the determination of the viscosity and the yield stress. Under site conditions, flowability can be judged by the consistency of the grout evaluated with various flow cone tests such as ASTM Test Method for Flow of Grout for Preplaced Aggregate Concrete (Flow Cone Method) (C 939) by determining indirectly the viscosity of the grout. Consistency tests are simple and useful on site, but they offer only rough descriptions of the relative flowability and neither gives separate values for the viscosity and the yield stress nor establishes a clear correlation between consistency and viscosity.

More accurate devices are various types of viscometers suitable for Newtonian or Bingham fluid grouting materials. The most well-known and commonly used is the coaxial cylinder viscometer. Many investigations have been conducted on various factors influencing the viscosity of cement paste. For instance, both Yang and Jennings (1995), as well as Williams et al. (1999) addressed the effects of mixing. Banfill (1999) and Saak et al. (1999) studied the effects of mix proportions and admixtures. Yang and Jennings (1999) also carried out the time dependency of viscosity during the induction period. The reason for this disagreement is that the rheological behavior of cement paste is very complex

because of the interaction of chemical and physical processes during setting and shearing. So far, no particular method for the viscosity testing of cement paste has been established satisfactorily. The condition is further aggravated by the use of different apparatus and procedures for mixing and testing.

Most of the previous works are comparative studies of particular factors, while prediction of the grouting process requires not only the trends of various effects on desirable flow properties, but also the magnitude of viscosity in the course of injection. Few studies in the past have been carried out on the shear history relevant to the construction processes. One attempt is by Chappuis (1996) who used a low measuring speed at 5 rpm for 5 s to simulate the low shearing rate and short duration for concrete placing. Saak et al. (1999) studied the rheological properties of cement paste for use in self-compacting concrete. The equilibrium viscosity at a constant shear rate was measured at 600 s^{-1}, considered to be an intermediate shear rate between the extremes of pouring and pumping. In this study, the viscosity test parameters, (e.g., the range and changing mode of the shear rate), were designed to simulate the shear history that the cement grout experienced during the flow of a preplaced aggregate grouting process.

Huang and Chen (2002) in order to reduce grouting costs, a new preparation technology for wet-ground fine cement (WFC) were developed. After grinding by this method, the maximum size of cement particles in slurry is not bigger than 40 mm and the medium size (50% by weight) is less than 10 mm; thus, the slurry can be used to inject a rock body with micro-fissures. This newly developed grouting technology with the special gear-grinder has been used successfully in some hydropower projects

in China such as Wan'an Project in Jiangxi province and the Three Gorges Project in Yichang city.

As the most commonly used grout material, ordinary Portland cement (OPC) has many advantages such as high strength, high durability, non-poison and low cost. But OPC can only be used to inject rock masses, in which breadth of fissure is bigger than 0.2 mm, because there are some large particles which maximum size is more than 80 mm. When the water/cement ratio of slurry is over 2:1, it is difficult to be injected into micro-fissures due to bad stability and bleeding. At the same time, because of bleeding and shrinkage of set grout, the viscous strength between hardened cement and grouted rock decreases, resulting in a new seepage route. To grout rock masses, especially that with micro-fissures, OPC cannot meet the requirements of projects, so developing fine or superfine cement has become increasingly important.

Park and Noh (2004) the rheological properties of cementitious materials containing fine particles, such as mineral admixtures (MA), were investigated using a Rotovisco RT 20 rheometer (Haake) with a cylindrical spindle. The mineral admixtures were finely ground blast furnace slag, fly ash and silica fume. The cementitious materials were designed as one, two and three components systems by replacement of ordinary Portland cement (OPC) with these mineral admixtures. The rheological properties of one-component system (OPC) were improved with increasing the dosage of PNS-based super plasticizer. For two-component systems, yield stress and plastic viscosity decreased with replacing OPC with blast furnace slag (BFS) and fly ash (FA). In the case of OPC-silica fume (SF) system, yield stress and plastic viscosity steeply increased with increasing SF. For three components

systems, both OPC-BFS-SF and OPC-FA-SF systems, the rheological properties improved, compared with the sample with SF. In the two and three components systems, the rheological properties of samples containing BFS improved much more than with FA replacement alone.

Schwartzentruber and Roy (2004) self-Compacting Concrete (SCC) has a high flowability and can be placed without vibration. It is defined as a concrete that exhibits a high deformability and a good resistance to segregation. This kind of concrete is of great interest and has gained wide use especially in the case of difficult casting conditions such as heavily reinforced sections. From a rheological point of view, the use of a Viscosity Enhancing Admixture (VEA) along with adequate super plasticizer content enables to ensure high deformability and stability. However, little is known about the interactions between super plasticizer and viscosity agent. Hence, we propose to study several cement pastes formulated from the original paste of a typical SCC mix. Depending on their rheological behavior, these pastes will be used later to study the stability of coarse aggregates. The major aim of this paper is to show that empirical tests such as spread and flow times are suitable to characterize the rheological behavior of cement pastes instead of more complex ones. Rheological properties, i.e. viscosity and shear yield stress, are well correlated with empirical test results in the range of flow able mixes. Moreover, the experimental program leads to emphasize the effects of the mixing procedure on the rhelogical properties of cement pastes. Finally, test results enable to underline the interactions between super plasticizer and Viscosity Enhancing Admixture used in designing Self Compacting Concrete.

Jarny et al, (2005) from MRI measurements, it is shown that in a flowing cement paste the thixotropic effects dominate over short time scales, while aging effects become significant over larger timescales. The steady state behavior, defined as flow properties in the intermediate period, exhibits a yielding behavior which differs from the prediction of usual yield stress models. The transition from the ''solid'' to the ''liquid'' regime is abrupt: the shear rate changes suddenly from zero to a finite value (critical shear rate) when the shear stress overcomes a critical value. These critical shear rates and shear stresses are independent of the flow conditions so that they may be considered as intrinsic material parameters. It was also shown that these results are consistent with usual macroscopic observations from conventional rheometry.

Emoto and Bier (2007) in the calcium aluminates cement – Portland cement – calcium sulfate based self-leveling underlayment, the influence of raw materials on the properties such as rheology and hydration kinetics was considered. It was confirmed that calcium aluminates cement system formulation is suitable in cases where a short open time is required, and Portland cement system formulation is suitable in cases where a long open time is required with the result of flowability or rheology. And, in order to thin the viscosity of slurry, it turned out that the application of MF 2651F as a plasticizer and tartaric acid as a retarder were effective. Moreover, MF 2651F seldom delayed the hydration reaction compared with other plasticizers. The flow value and the yield stress showed correlation, without being dependent on the difference in formulation or a water powder ratio. This was considered to be because for the yield stress to relate to the fragility of the aggregation structure of slurry.

2.2.2 Strength of cured grout

Tango (1998) compressive strength is the most important concrete property because it is the main parameter for quality control. Also, for cements, quality is assessed by testing cylindrical, cubic, or prismatic standard mortar specimens under compressive stress. Several methods have been proposed for predicting the strength of cement paste, mortar, or concrete at the control age (usually 28 days) from measurements at earlier ages. Such methods give the predicted strength based on a group of cement or concrete characteristics. They can be classified as:

1. Accelerated Curing Methods: The hardening hydration reactions of cement are accelerated by heating the specimens under normal or high pressure or using accelerating admixtures. Previously developed equations correlating specimen strengths with and without the acceleration process are necessary.

2. Correlations with Early Age Strengths Under Standard Curing Conditions: The test results obtained on specimens at an early age (e.g., 3 or 7 days) are previously related to the corresponding value at the control age (e.g., 28 days) by regression analysis, and the resulting equation is used for the prediction.

3. Correlation Methods Using Other Characteristics: This large group of methods includes correlations between the control age strength and chemical composition and fineness of cement, porosity estimated from fresh mixture air content and water-cement ratio, measured heat of hydration, and early-age sonic pulse velocity (1,2); it also includes the prediction with basis as the measured compressive strength with a known maturity at an early age and its projection using a previous strength–maturity equation.

All these methods require previous experimental correlations obtained with the same materials and conditions of the particular controlled job.

The present method is based on experiments carried out since 1990 and classified approximately into Category 2, with the difference that they do not use a correlation with early age strengths, but extrapolate the control age strength after obtaining two earlier age strengths in the strength-time diagram, with axes adequately transformed to linearize the original curve. This extrapolation has shown independence of a large number of variables which are not negligible in other prediction methods.

Duval and Kadri (1998) the workability and the compressive strength of silica fume concretes were investigated at low water-cementitious materials ratios with a naphthalene sulphonate super plasticizer. The results show that partial cement replacement up to 10% silica fume does not reduce the concrete workability. Moreover, the super plasticizer dosage depends on the cement characteristics (C3A and alkali sulfates content). At low water-cementitious materials ratios, slump loss with time is observed and increases with high replacement levels. Silica fume at replacement contents up to 20% produce higher compressive strengths than control concretes; nevertheless, the strength gain is less than 15%. In this paper, we propose a model to evaluate the compressive strength of silica fume concrete at any time. The model is related to the water-cementitious materials and silica-cement ratios. Taking into account the author's and other researchers' experimental data, the accuracy of the proposed model is better than 5%. Figure 2.1 Shows the strength development of concretes at different water-cementitious materials ratios.
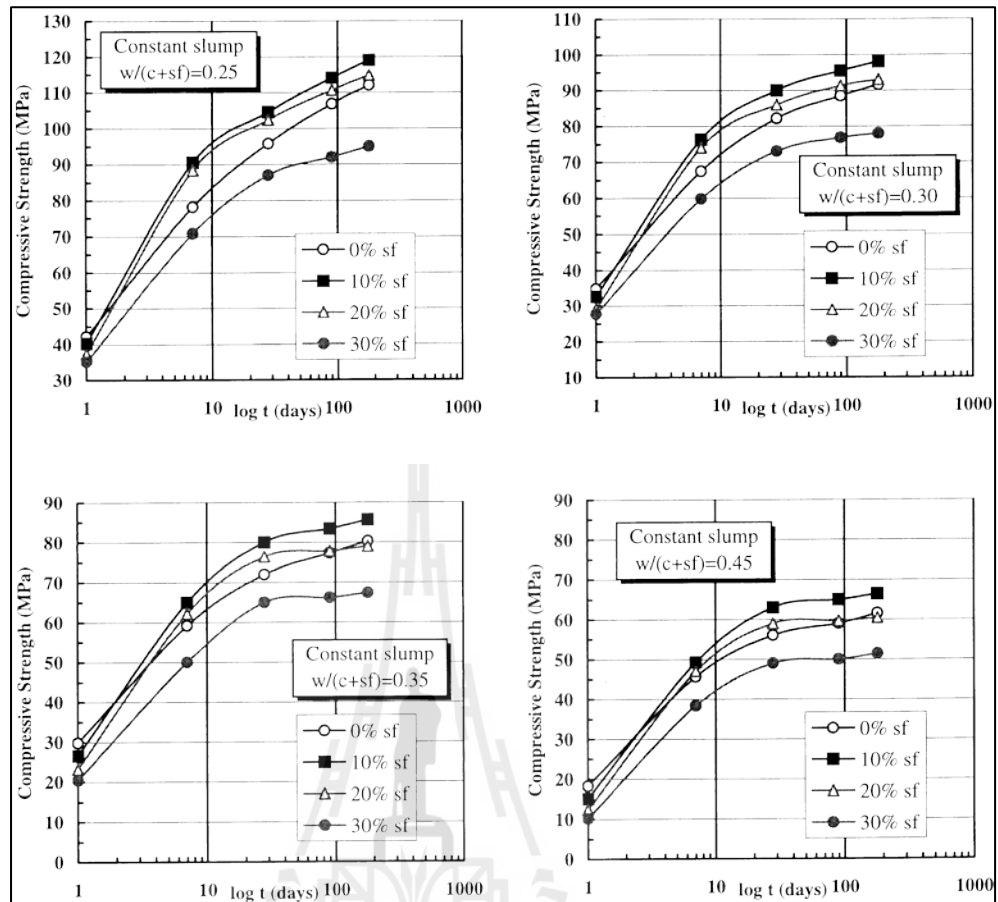
Figure 2.1 Strength developments of concretes at different water-cementitious materials ratios.

Shannag and Haddad (2005) cement based grouts containing 0, 5, 10, and 15 % replacement with metakaolin and with a water/cementitious materials ratio of 0.38 have been investigated. The rheological and mechanical properties of the proposed grouts are interesting, since, from a practical point of view, they exhibit no bleeding or segregation and reach high compressive strength and flowability. Metakaolin additions enhanced the strength, somewhat prolonged the setting times, reduced the flowability, improved sulfate resistance, and caused some increase in drying

shrinkage. The results showed that Metakaolin could be added up to 15 % by weight of cement without reducing the 28-day strength. At 15 % admixing level, strength of the grout at the age of 28 days was increased by about 10 %. Based on the test results the use of Metakaolin for producing high-strength cementitious grouts is recommended.

Considering the relative importance of compressive strength in cement and concrete technology, the compressive strength of the grouts was measured on 75 mm × 150 mm cylinders that were cast and cured in steel molds. Strength measurements for grouts cured in water were conducted at ages of 7 and 28 days.

The compressive strength of the grout is a property that relates to the structure of the cement paste and provides an indicator of its quality. As expected, the hardened grouts developed high-early compressive strength. After 28 days, it was around 55.5 MPa. The highest compressive strengths were observed for the grout containing 15 % MK as shown in Table 2.1. It is observed that adding up to 15 % MK caused about 10 % increase in 28 days strength. The increase in strength of the grouts containing MK is probably the result of a combined filler and pozzolanic effect. The filler effect leads to reduction in porosity of the transition zone and provides a dense microstructure and thus increases the strength of the grout. The pozzolanic effect helps in the formation of bonds between the densely packed particles in the transition zone through the pozzolanic reaction with the calcium hydroxide liberated during the hydration of Portland cement to form extra binding calcium silicates hydrates, which leads to further increase in strength.

Table 2.1 Compressive strength of the grouts proposed.

Metakaolin Content (%)	Uniaxial Compressive Strength, σ_c (MPa)	
	7 days	28 days
0 (OPC)	45.30	50.30
5	44.40	52.10
10	46.20	52.40
15	49.50	55.50

James and Cheng (2011) a trial pressure grouting program is conducted to restore the load carrying capabilities of Portland cement concrete slabs that have been in service for a number of years and are showing signs of distress. First, a series of laboratory tests are conducted to find a Portland cement grout mix with the appropriate properties of fluidity, viscosity, stability, shrinkage, and strength. Type I cement was used to prepare three grout mixtures having water-to-cement ratios of 0.6, 0.8, and 1.0. Super plasticizer was added at a dosage of 2%, 5%, and 8%, by mass of cement, Grout specimens with a diameter of 5 mm and a height of 10 mm were tested in unconfined compression up to 7 days of curing. All specimens were loaded in displacement control tests at a rate of 0.15 mm/min on a servo-hydraulic closed loop, which were trimmed and capped to ensure smooth and parallel ends. The variation in the compressive strength of cement grout with variable mixes is displayed in Figure 2.2 versus curing time.
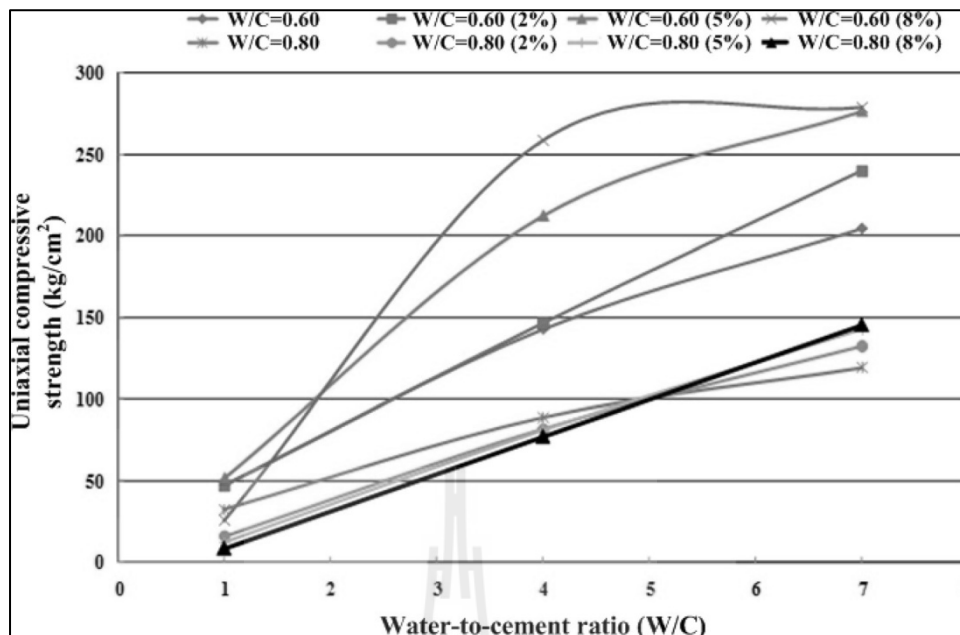
Figure 2.2 Strength and curing time relationship for cement grout with variable

mixes.

2.2.3 Permeability of the grout

Halamickova and Detwiler (1995) the pore structure of hydrated cement in

mortar and concrete is quite different from that of neat cement paste. The porous

transition zones formed at the aggregate-paste interfaces affect the pore size

distribution. The effect of the sand content on the development of pore structure, the

permeability to water, and the diffusivity of chloride ions was studied on Portland

cement mortars. Mortars of two water-to-cement ratios and three sand volume

fractions were cast together with pastes and tested at degrees of hydration ranging

from 45 to 70%. An electrically-accelerated concentration cell test was used to

determine the coefficient of chloride ion diffusion while a high pressure permeability

cell was employed to assess liquid permeability. The coefficient of chloride ion

diffusion varied linearly with the critical pore radius as determined by mercury intrusion porosimetry while permeability was found to follow a power-law relationship vs. this critical radius. The data set provides an opportunity to directly examine the application of the Katz-Thompson relationship to cement-based materials.

Christensen et al. (1996) the experimental and calculated permeability of hardened cement pastes were compared. Experimental data for water permeability was obtained from the work of Nyame and Illston in 1980 on neat pastes with water-to-cement ratios (w/c) between 0.23 and 1.0. Mercury intrusion porosimetry (MIP) and impedance spectroscopy (IS) measurements were performed on equivalently prepared specimens. Then the Katz-Thompson relation was used to calculate permeability. Calculated results track well with experimental data as a l&ction of time, with the experimental value of permeability slightly higher at most times. The correlation between experimental and calculated permeability, at all times, are within 1.5 orders of magnitude. The largest differences occurred at late times for the samples with low w/c ratio. This calculated permeability is quick, relatively simple and appears to give reasonable results when compared to conventional water intrusion methods.

Valenza and Thomas (2011) the permeability and elastic modulus of mature cement paste cured at temperatures between 8 °C and 60 °C were measured using a previously described beam bending method. The permeability increases by two orders of magnitude over this range, with most of the increase occurring when the curing temperature increases from 40 °C to 60 °C. The elastic modulus varies much less, decreasing by about 20% as the curing temperature increases from 20 °C to 60 °C.

All specimens had very low permeability, kb0.1 nm2, despite having relatively high porosity, ϕ ~40%. Concomitant investigations of the microstructure using small angle neutron scattering and thermoporometry indicate that the porosity is characterized by nanometric pores, and that the characteristic size of pores controlling transport increases with curing temperature. The variation of the microstructure with curing temperature is attributed to changes in the pore structure of the calcium–silicate–hydrate reaction product. Both the empirical Carmen–Kozeny, and modified Carmen–Kozeny permeability models suggest that the tortuosity is very high regardless of curing temperature, ξ ~1000.

Wong et al. (2011) a method to estimate permeability of cement-based materials using pore areas and perimeters from SEM images is presented. The pore structure is idealized as a cubic lattice having pores of arbitrary size. The hydraulic conductance of each pore is calculated using the hydraulic radius approximation, and a stereological factor is applied to account for the random orientation of the image plane. A 'constriction factor' is applied to account for variations in pore radius along the pore axis. Kirkpatrick's effective medium equation is then used to obtain an effective pore conductance, from which the macroscopic permeability is derived. The method was tested on forty-six pastes and mortars with different w/c ratio, cement, age and sand content. The permeability ranged from $3\times10^{-18}\text{m}^2$ to 5.8×10^{-16} m^2. It was found that 76% of the permeability was predicted to within a factor of ±2 and 98% within a factor of ±5 from measured values.

2.2.4 Experimental researches on cement and rock fracture

Akgüna and Daemen (1999) the strength measures of expansive cement grout borehole plugs cast in welded tuff cylinders is investigated as a function of the degree of saturation of the plugged rock cylinder and of borehole size. Details on experimental procedure regarding rock cylinder and cement grout preparation, sample curing conditions, experimental apparatus, sample loading, mechanical characterization of the rock, and cement grout, along with procedures for the determination of the sample saturation assuming uniform saturation, and strength measures are presented. The extrapolated axial strengths to a plug radius of 100 mm show that the more saturated samples show higher strengths as compared to the dry samples. The strength measures decrease with increasing plug radius, obeying a power law. Figure 2.3 Show the push out test apparatus.

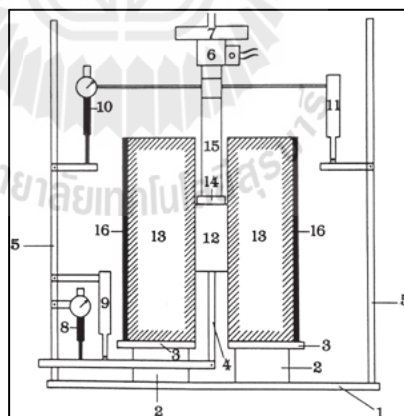**Figure 2.3.** Schematic drawing of push-out test setup. 1. Cylindrical steel plate, 2. Circular steel plate with a slit, 3. Square steel plate, 4. L-shaped steel rod, 5. Vertical steel rods, 6. Load cell, 7. Loading platen, 8, 10. Dial gages, 9,

11. LVDTs, 12. Cement grout plug, 13. Rock sample, 14. Steel cylinder, 15. Axial bar, 16. Steel pipe.

Fransson (2001) describes a rock volume suitable for a grouting field test at the Äspö Hard Rock Laboratory, Sweden. Fixed interval length transmissivities and the corresponding number of fractures from geological mapping of a probe hole were used to calculate a probability of conductive fractures for analyses of data from individual boreholes. The transmissivity and specific capacity of the boreholes were compared to examine the robustness of the specific capacity. From the findings of the study, the probability of conductive fractures from probe hole data, the specific capacity and fracture frequency of individual boreholes were sufficient to construct a simplified model of the fracture and the rock volume. The median specific capacity of the boreholes was a good description of the effective cross-fracture transmissivity. The field test was also carried out to demonstrate the usefulness of the methodology for improving the analyses of data from the hydraulic tests and geological mapping for a grouting fan.

Seidel1 and Haberfield (2002) describes the experimental component of an extensive investigation into the shear behavior of joints formed between concrete or cement grout and soft, weak or weathered rock. Understanding the behavior of such joints is important for the prediction of performance of a diverse range of structural elements, such as drilled piers socketed into rock, rock anchors, and dam foundations. The particular tests described in this paper were carried out on joints formed between concrete and an artificial siltstone called Johnstone, under conditions of constant normal stiffness, and involved a range of boundary conditions and interface profiles.

Figure 2.4 Show the schematic section of load application system of CNS device. Interfaces included a series of regular triangular asperities and irregular profiles based on fractal geometry concepts. The authors have included the complete suite of test results in the belief that it will be a significant addition to the literature, which currently contains very few results of constant normal stiffness tests. It also demonstrates the importance of realistically modeling interface roughness. Careful observations made during testing using time-lapse photography have aided in the development of a number of simple theoretical models of behavior, which are published elsewhere.
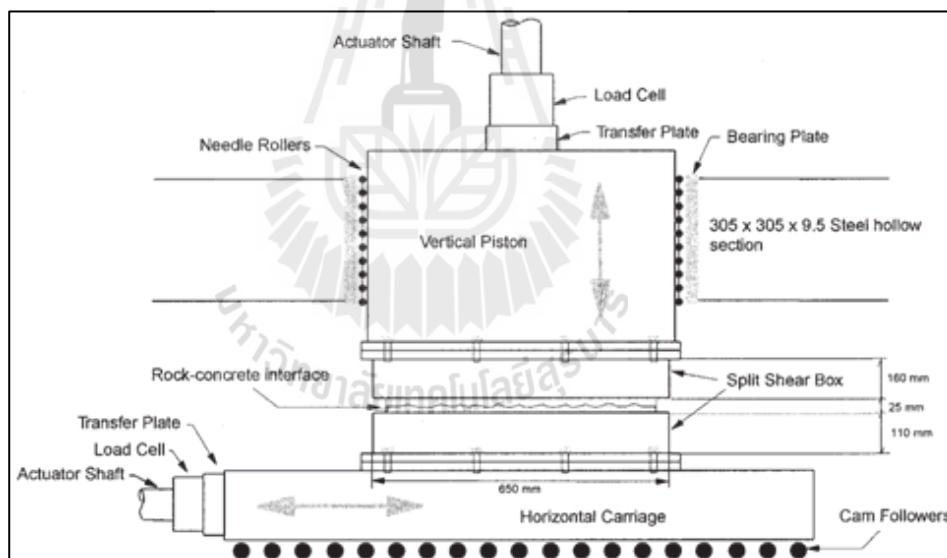

Figure 2.4. Schematic section of load application system of CNS device.

Rahmani (2004) explained that grouting had been used over the past two centuries to increase the strength, decrease the deformation and reduce the permeability of soils or fractured rocks. Due to its significance in engineering and

science predicting grout effectiveness in fractured rocks was of interest. There were different approaches to estimate the effectiveness of grouting, one of which was numerical modeling. Numerical models could simulate a distribution of grout inside fractures by which the effectiveness of grout could be estimated. Few numerical studies had been carried out to model grout penetration in fractured rocks. Due to complexities of modeling grout and fracture most of these studies had either used simplifying assumptions or been bound to small sizes of fractures, both resulting in unrealistic simulations.

Then the current work is aimed to eliminate some of the simplifying assumptions and to develop a model that could improve the reliability of the results. In reality, grouts were believed to behave as a Bingham fluid, but many models did not consider a full Bingham fluid flow solution due to its complexity. Real fractures had rough surfaces with randomly varying apertures. However, some models considered fractures as planes with two parallel sides and a constant aperture. In this work the Bingham fluid flow equations were solved numerically over a stochastically varying aperture fracture. To simplify the equations and decrease the computational time the current model substituted two-dimensional elements by one-dimensional pipes with equivalent properties. The model was capable of simulating the time penetration of grout in a mesh of fracture over a rather long period of time. The results of the model could be used to predict the grout penetration for different conditions of fractures or grout (Rahmani, 2004).

Varol and Dalgıc (2005) the first stage of the Istanbul metro construction was conducted in sandstone and mudstones of Carboniferous age. On the basis of Lugeon tests, the rock mass permeability was found to be in the range of 10^{-5}–10^{-7}. Since, no

waterproofing system was placed in between the primary support and the final lining to maintain the imperviousness during operation of the subway, the cracking of the concrete lining and water inflow problems, such as leakage through the repair, dripping and surface moisture caused difficulties for the operation of the metro system. In order to overcome these problems, three different contact grouting methods, repair grouting and chemical grouting works were carried out. Regarding homogeneity of the grout take, labor and time-dependency of the equipment, the most successful results were obtained from one of the contact grouting types and repair grouting. Chemical grouting works yielded unsatisfactory results. Moreover, alteration, fracture spacing, groundwater and excess excavation properties of the rock mass were investigated in comparison with the contact grout take. The comparison between these properties and the grout take indicates no close relationship, and the grout take values are found to be affected mainly by the labor of grouting and excavation. In addition, in order to improve the rock mass along the metro route, consolidation grouting works were conducted. However, grouting works with the use of Portland cement conducted in the rock mass of very low permeability do not yield successful results.

CHAPTER III

CEMENT GROUTS AND ROCK SPECIMENS

3.1   Cement grouts

The grouting materials in this study are ordinary Portland cement ASTM (C150) type 1 obtained from five cement suppliers in Thailand, including (1) Asia Cement Public Company Limited (ACC), (2) CEMEX Thailand Cement Public Company Limited (CEMEX), (3) Siam Cement Group Public Company Limited (SCG), (4) Siam City Cement Public Company Limited (SCCC), and (5) TPI Polene Cement Public Company Limited (TPI). The chemical compositions and some physical characteristics of these materials are given in Table 3.1. All grouts are prepared by mixing at the water-to-cement ratio of 0.60 (James and Cheng, 2011).

The grout preparation follows the ASTM (C938) standard practice using a Hobart type laboratory mixer (Figure 3.1). The cement slurry mixtures are poured and cured in 54 mm diameter PVC pipes for the mechanical testing. Figure 3.2 shows the specimens cured under distilled water at room temperature (ASTM C192) before testing. A total of 225 specimens of five cement supplier are prepared for basic mechanical properties testing. Some specimens are shown in Figure 3.3. Table 3.2 summarizes the specimen number, dimensions, and density.

Table 3.1 Typical chemical compositions of ordinary Portland cement type I

   (ASTM C150).

Compositions	(%)
Silicon dioxide (SiO_2)	20.9
Aluminum oxide (Al_2O_3)	5.6
Ferric oxide (Fe_2O_3)	3.1
Calcium oxide (CaO)	62.7
Magnesium oxide (MgO)	2.2
Sodium oxide (Na_2O)	0.2
Potassium oxide (K_2O)	0.8
Sulfur trioxide (SO_3)	2.9
Loss on Ignition (%)	1.3
Specific Gravity	3.15
Specific Surface (m^2/kg)	300

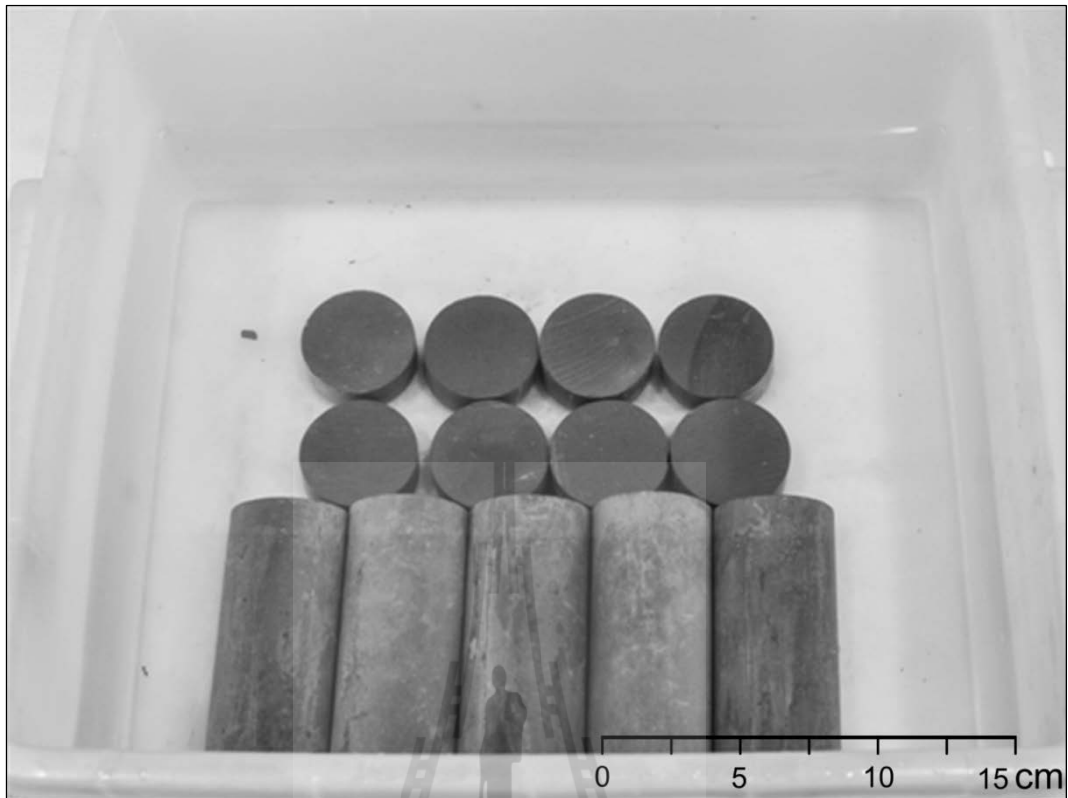**Figure 3.1** Hobart type laboratory mixer used to prepare cement grout.

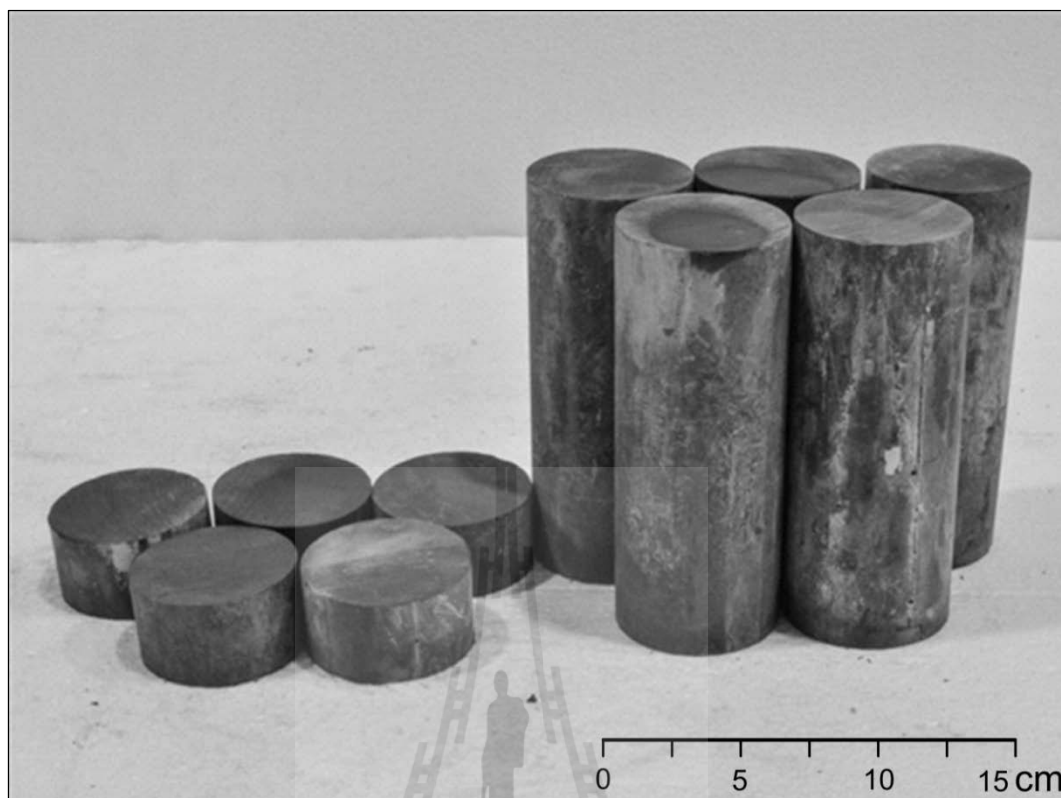**Figure 3.2** Cement grout specimens cured under distilled water.

Figure 3.3 Some specimens prepared for basic mechanical properties testing.
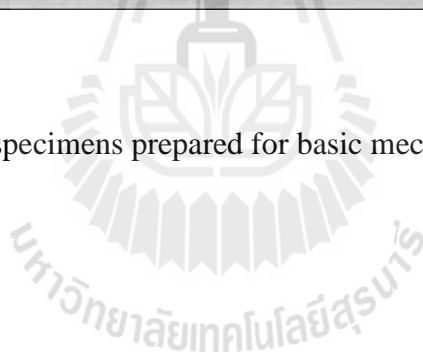
Table 3.2 Specimen dimensions after preparation.

Specimen No.	Diameter (mm.)	Height (mm.)	Density (g/cc)
ACC-UCS-03-1	54.00	134.30	1.69
ACC-UCS-03-2	54.60	134.70	1.70
ACC-UCS-03-3	53.84	134.00	1.73
ACC-UCS-03-4	53.74	135.40	1.75
ACC-UCS-03-5	54.62	133.90	1.69
ACC-UCS-07-1	53.64	134.96	1.74
ACC-UCS-07-2	53.74	135.42	1.78
ACC-UCS-07-3	54.52	134.62	1.75
ACC-UCS-07-4	53.30	134.72	1.76
ACC-UCS-07-5	53.60	134.02	1.80
ACC-UCS-14-1	53.62	137.46	1.78
ACC-UCS-14-2	54.20	136.00	1.80
ACC-UCS-14-3	53.80	138.12	1.80
ACC-UCS-14-4	54.00	136.80	1.81
ACC-UCS-14-5	54.00	137.00	1.81
ACC-UCS-28-1	53.84	136.74	1.82
ACC-UCS-28-2	53.42	136.24	1.84
ACC-UCS-28-3	53.26	135.88	1.85
ACC-UCS-28-4	53.26	135.98	1.84
ACC-UCS-28-5	53.78	135.82	1.82
CEMEX-UCS-03-1	53.94	135.20	1.77
CEMEX-UCS-03-2	53.84	135.40	1.74
CEMEX-UCS-03-3	53.94	135.40	1.75
CEMEX-UCS-03-4	54.30	135.42	1.76
CEMEX-UCS-03-5	53.24	135.52	1.78
CEMEX-UCS-07-1	53.54	135.00	1.79
CEMEX-UCS-07-2	54.12	134.42	1.73
CEMEX-UCS-07-3	53.52	134.00	1.78
CEMEX-UCS-07-4	53.36	134.32	1.81
CEMEX-UCS-07-5	53.84	134.82	1.81
CEMEX-UCS-14-1	53.74	135.70	1.82
CEMEX-UCS-14-2	53.96	137.60	1.80
CEMEX-UCS-14-3	50.80	136.00	1.82
CEMEX-UCS-14-4	53.78	136.48	1.81
CEMEX-UCS-14-5	53.90	137.70	1.84
CEMEX-UCS-28-1	53.38	136.64	1.84
CEMEX-UCS-28-2	53.44	135.78	1.84
CEMEX-UCS-28-3	53.82	135.12	1.82

Table 3.2 Specimen dimensions after preparation (continue).

Specimen No.	Diameter (mm.)	Height (mm.)	Density (g/cc)
CEMEX-UCS-28-4	53.02	135.16	1.87
CEMEX-UCS-28-5	53.16	135.03	1.86
SCG-UCS-03-1	51.02	136.64	1.77
SCG-UCS-03-2	50.84	135.58	1.79
SCG-UCS-03-3	51.48	135.00	1.78
SCG-UCS-03-4	51.38	135.00	1.78
SCG-UCS-03-5	51.20	135.12	1.78
SCG-UCS-07-1	51.30	134.70	1.75
SCG-UCS-07-2	51.00	135.00	1.75
SCG-UCS-07-3	51.02	136.68	1.75
SCG-UCS-07-4	51.18	134.72	1.75
SCG-UCS-07-5	51.00	134.00	1.76
SCG-UCS-14-1	53.30	134.38	1.78
SCG-UCS-14-2	54.00	134.48	1.78
SCG-UCS-14-3	53.02	135.80	1.78
SCG-UCS-14-4	51.00	134.18	1.78
SCG-UCS-14-5	50.80	136.78	1.80
SCG-UCS-28-1	53.74	135.68	1.79
SCG-UCS-28-2	53.90	134.00	1.80
SCG-UCS-28-3	51.08	136.00	1.78
SCG-UCS-28-4	53.90	136.48	1.77
SCG-UCS-28-5	53.78	134.55	1.80
SCCC-UCS-03-1	54.00	135.00	1.80
SCCC-UCS-03-2	53.32	135.32	1.81
SCCC-UCS-03-3	54.12	135.66	1.80
SCCC-UCS-03-4	53.82	135.82	1.79
SCCC-UCS-03-5	53.74	134.86	1.80
SCCC-UCS-07-1	53.44	135.02	1.84
SCCC-UCS-07-2	53.36	135.38	1.84
SCCC-UCS-07-3	54.02	135.28	1.80
SCCC-UCS-07-4	53.62	136.02	1.82
SCCC-UCS-07-5	54.04	135.28	1.80
SCCC-UCS-14-1	53.67	136.14	1.86
SCCC-UCS-14-2	53.26	137.30	1.85
SCCC-UCS-14-3	53.71	135.54	1.86
SCCC-UCS-14-4	53.50	135.90	1.85
SCCC-UCS-14-5	53.46	135.90	1.85
SCCC-UCS-28-1	53.94	135.00	1.81

Table 3.2 Specimen dimensions after preparation (continue).

Specimen No.	Diameter (mm.)	Height (mm.)	Density (g/cc)
SCCC-UCS-28-2	53.34	134.90	1.88
SCCC-UCS-28-3	53.50	133.20	1.85
SCCC-UCS-28-4	53.30	135.50	1.88
SCCC-UCS-28-5	53.84	135.14	1.84
TPI-UCS-03-1	54.16	136.68	1.77
TPI-UCS-03-2	51.14	136.38	1.76
TPI-UCS-03-3	51.08	135.40	1.79
TPI-UCS-03-4	51.28	136.00	1.75
TPI-UCS-03-5	53.44	136.28	1.76
TPI-UCS-07-1	54.40	134.48	1.78
TPI-UCS-07-2	50.90	135.80	1.81
TPI-UCS-07-3	51.10	134.44	1.77
TPI-UCS-07-4	51.10	134.80	1.79
TPI-UCS-07-5	51.50	133.70	1.76
TPI-UCS-14-1	54.30	133.70	1.77
TPI-UCS-14-2	51.34	134.70	1.77
TPI-UCS-14-3	51.10	134.80	1.77
TPI-UCS-14-4	51.54	133.50	1.78
TPI-UCS-14-5	53.20	138.20	1.77
TPI-UCS-28-1	51.52	135.86	1.77
TPI-UCS-28-2	51.46	135.26	1.75
TPI-UCS-28-3	51.06	135.00	1.81
TPI-UCS-28-4	51.28	135.42	1.76
TPI-UCS-28-5	51.26	134.72	1.80
ACC-BZ-03-1	53.90	30.20	1.78
ACC-BZ-03-2	54.40	28.84	1.79
ACC-BZ-03-3	54.10	30.20	1.79
ACC-BZ-03-4	53.64	29.32	1.78
ACC-BZ-03-5	53.54	29.00	1.78
ACC-BZ-07-1	54.02	28.44	1.78
ACC-BZ-07-2	53.64	27.58	1.78
ACC-BZ-07-3	53.24	27.66	1.79
ACC-BZ-07-4	53.64	28.84	1.78
ACC-BZ-07-5	54.42	28.24	1.77
ACC-BZ-14-1	53.78	29.10	1.79
ACC-BZ-14-2	54.22	30.70	1.79
ACC-BZ-14-3	54.10	28.60	1.81
ACC-BZ-14-4	54.30	28.30	1.80

Table 3.2 Specimen dimensions after preparation (continue).

Specimen No.	Diameter (mm.)	Height (mm.)	Density (g/cc)
ACC-BZ-14-5	54.00	28.20	1.80
ACC-BZ-28-1	53.24	27.98	1.80
ACC-BZ-28-2	53.68	28.02	1.80
ACC-BZ-28-3	54.12	28.36	1.81
ACC-BZ-28-4	53.26	28.34	1.81
ACC-BZ-28-5	53.66	28.46	1.80
CEMEX-BZ-03-1	53.60	28.34	1.78
CEMEX-BZ-03-2	53.64	29.84	1.78
CEMEX-BZ-03-3	53.14	29.42	1.78
CEMEX-BZ-03-4	53.84	28.84	1.77
CEMEX-BZ-03-5	53.74	28.86	1.77
CEMEX-BZ-07-1	54.00	28.28	1.79
CEMEX-BZ-07-2	53.34	28.32	1.79
CEMEX-BZ-07-3	53.12	28.12	1.78
CEMEX-BZ-07-4	53.92	28.02	1.80
CEMEX-BZ-07-5	54.18	28.56	1.79
CEMEX-BZ-14-1	54.62	28.90	1.80
CEMEX-BZ-14-2	54.32	28.44	1.79
CEMEX-BZ-14-3	53.14	28.24	1.79
CEMEX-BZ-14-4	54.64	29.00	1.79
CEMEX-BZ-14-5	53.72	27.48	1.80
CEMEX-BZ-28-1	51.68	27.12	1.79
CEMEX-BZ-28-2	51.76	27.46	1.80
CEMEX-BZ-28-3	53.42	28.28	1.80
CEMEX-BZ-28-4	53.86	28.34	1.80
CEMEX-BZ-28-5	53.62	29.02	1.80
SCG-BZ-03-1	54.30	29.00	1.82
SCG-BZ-03-2	54.72	29.82	1.83
SCG-BZ-03-3	53.24	28.82	1.84
SCG-BZ-03-4	54.48	29.08	1.84
SCG-BZ-03-5	53.62	29.54	1.80
SCG-BZ-07-1	50.80	29.72	1.84
SCG-BZ-07-2	54.24	28.52	1.82
SCG-BZ-07-3	53.94	30.00	1.82
SCG-BZ-07-4	54.00	30.00	1.80
SCG-BZ-07-5	51.30	29.22	1.84
SCG-BZ-14-1	51.28	29.00	1.82
SCG-BZ-14-2	51.30	29.22	1.84

Table 3.2 Specimen dimensions after preparation (continue).

Specimen No.	Diameter (mm.)	Height (mm.)	Density (g/cc)
SCG-BZ-14-3	54.12	29.72	1.83
SCG-BZ-14-4	52.88	29.40	1.83
SCG-BZ-14-5	54.94	28.50	1.82
SCG-BZ-28-1	53.04	29.48	1.81
SCG-BZ-28-2	51.16	29.42	1.82
SCG-BZ-28-3	51.00	29.68	1.91
SCG-BZ-28-4	51.46	29.48	1.83
SCG-BZ-28-5	51.12	29.48	1.83
SCCC-BZ-03-1	54.02	28.12	1.80
SCCC-BZ-03-2	54.18	30.00	1.81
SCCC-BZ-03-3	53.82	28.14	1.81
SCCC-BZ-03-4	53.68	28.82	1.78
SCCC-BZ-03-5	54.00	28.00	1.81
SCCC-BZ-07-1	54.14	27.50	1.83
SCCC-BZ-07-2	53.48	27.46	1.80
SCCC-BZ-07-3	54.44	28.72	1.80
SCCC-BZ-07-4	54.22	28.58	1.82
SCCC-BZ-07-5	54.12	28.28	1.81
SCCC-BZ-14-1	54.00	27.70	1.83
SCCC-BZ-14-2	54.40	28.02	1.78
SCCC-BZ-14-3	54.12	27.72	1.82
SCCC-BZ-14-4	53.80	29.70	1.79
SCCC-BZ-14-5	54.46	26.74	1.80
SCCC-BZ-28-1	53.94	27.40	1.82
SCCC-BZ-28-2	53.64	29.02	1.80
SCCC-BZ-28-3	53.70	26.28	1.81
SCCC-BZ-28-4	54.20	28.00	1.80
SCCC-BZ-28-5	53.40	30.02	1.80
TPI-BZ-03-1	54.18	30.00	1.76
TPI-BZ-03-2	54.00	29.58	1.77
TPI-BZ-03-3	51.28	29.10	1.76
TPI-BZ-03-4	54.30	29.22	1.77
TPI-BZ-03-5	53.50	30.30	1.76
TPI-BZ-07-1	51.48	29.22	1.78
TPI-BZ-07-2	51.44	28.00	1.77
TPI-BZ-07-3	51.30	28.26	1.76
TPI-BZ-07-4	51.28	28.14	1.77
TPI-BZ-07-5	51.58	28.24	1.78

Table 3.2 Specimen dimensions after preparation (continue).

Specimen No.	Diameter (mm.)	Height (mm.)	Density (g/cc)
TPI-BZ-14-1	53.70	27.80	1.78
TPI-BZ-14-2	54.50	28.20	1.79
TPI-BZ-14-3	53.64	27.88	1.78
TPI-BZ-14-4	51.00	29.18	1.78
TPI-BZ-14-5	54.22	29.70	1.78
TPI-BZ-28-1	54.32	28.00	1.79
TPI-BZ-28-2	53.40	27.88	1.78
TPI-BZ-28-3	54.06	28.54	1.77
TPI-BZ-28-4	54.30	28.26	1.77
TPI-BZ-28-5	54.12	28.22	1.79
ACC-TCS-28-1	54.10	105.00	1.83
ACC-TCS-28-2	53.80	107.00	1.83
ACC-TCS-28-3	53.70	106.56	1.81
ACC-TCS-28-4	53.34	104.12	1.82
ACC-TCS-28-5	53.54	104.48	1.83
CEMEX-TCS-28-1	53.64	109.70	1.80
CEMEX-TCS-28-2	53.62	108.98	1.81
CEMEX-TCS-28-3	53.60	108.00	1.81
CEMEX-TCS-28-4	53.84	109.06	1.80
CEMEX-TCS-28-5	53.74	109.12	1.80
SCG-TCS-28-1	54.32	110.00	1.82
SCG-TCS-28-2	54.00	109.62	1.81
SCG-TCS-28-3	54.00	108.00	1.82
SCG-TCS-28-4	53.50	110.00	1.82
SCG-TCS-28-5	53.14	109.90	1.82
SCCC-TCS-28-1	54.00	111.08	1.81
SCCC-TCS-28-2	54.00	111.00	1.81
SCCC-TCS-28-3	53.90	109.38	1.82
SCCC-TCS-28-4	54.14	111.00	1.81
SCCC-TCS-28-5	54.00	110.40	1.81
TPI-TCS-28-1	54.00	108.00	1.82
TPI-TCS-28-2	53.00	108.30	1.82
TPI-TCS-28-3	53.00	108.00	1.83
TPI-TCS-28-4	53.84	108.72	1.82
TPI-TCS-28-5	53.00	108.64	1.81

3.2   Rock specimens

The fractures in rock cylinders are artificially by line loading in Phu Kradung sandstone blocks. These fine-grained rocks have highly uniform texture. Figure 3.4 through 3.5 shows rock samples used for the four point bending test prepared by applying a line load at the center to induce a splitting tensile crack in 54 mm diameter, 200 mm long cylindrical specimens. Over twenty specimens are prepared for this test. The specimens for push out test are rectangular sandstone block with a hole drilled through the center of the specimen with a diameter of 34 mm. Figure 3.6 through 3.7 shows the specimens prepared for the push out test.
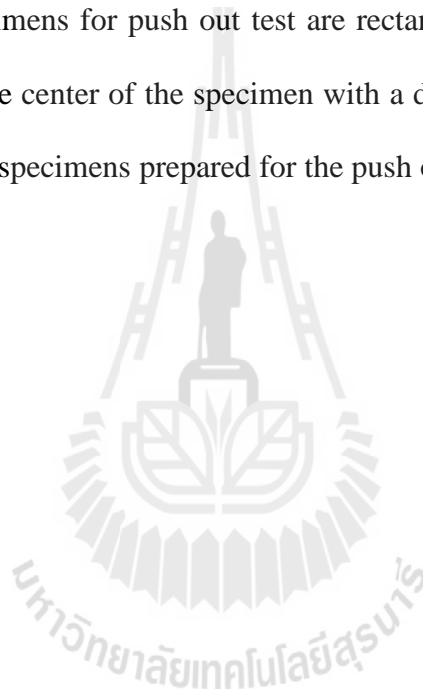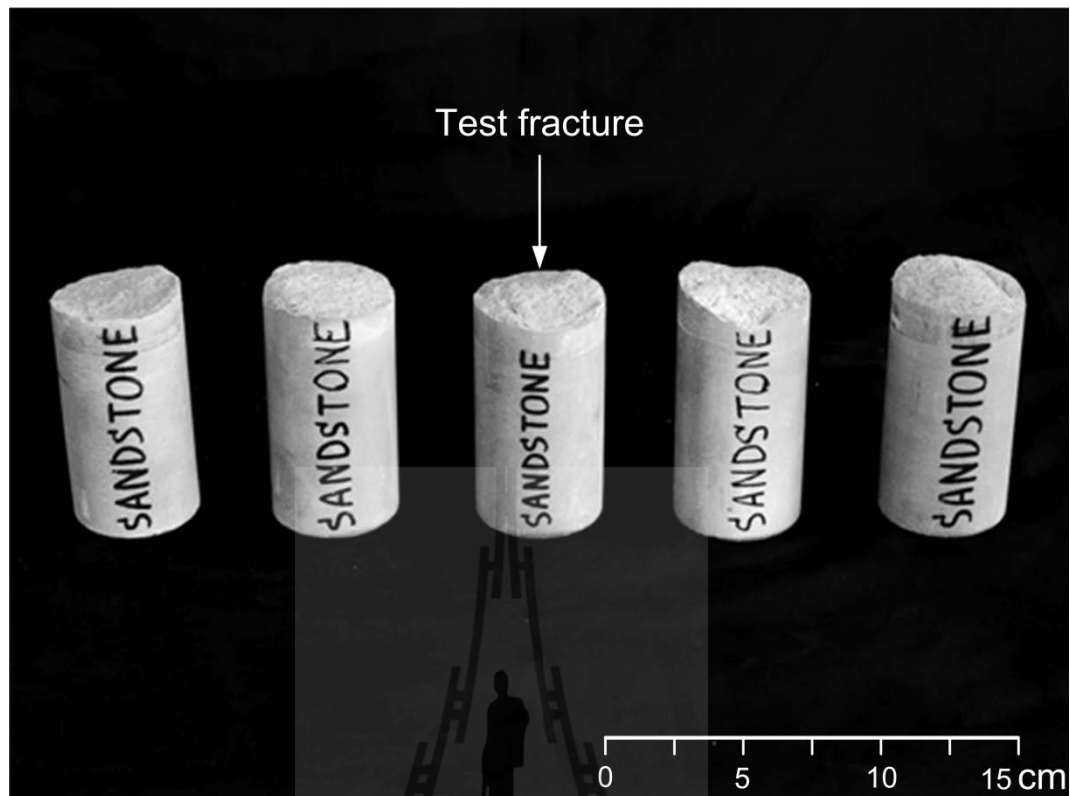
Figure 3.4 Phu Kradung sandstone specimens prepared for four point bending test.
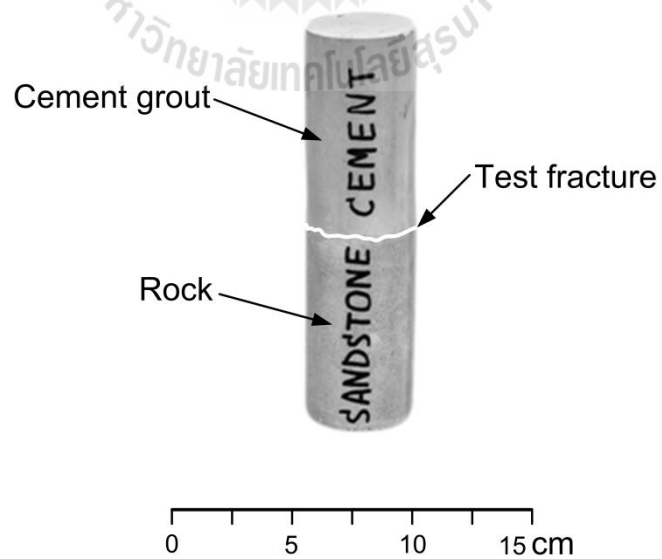
Figure 3.5 The specimens prepared for four point bending test.
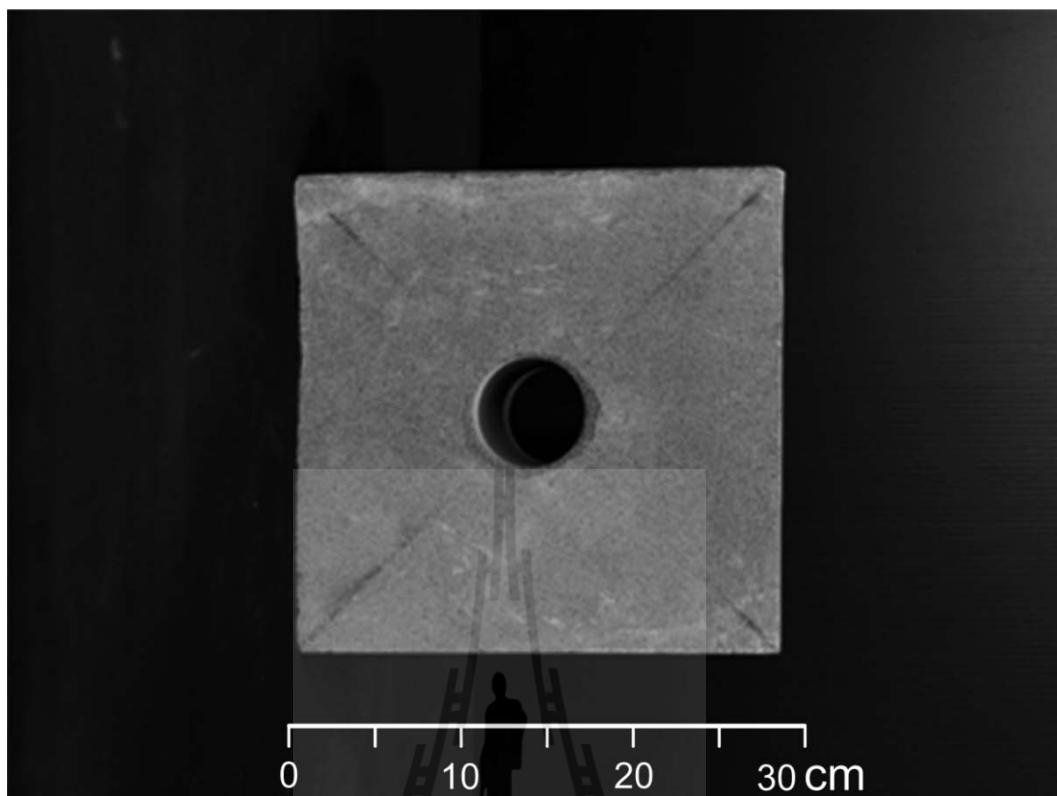
Figure 3.6 Phu Kradung sandstone specimens prepared for push out test.
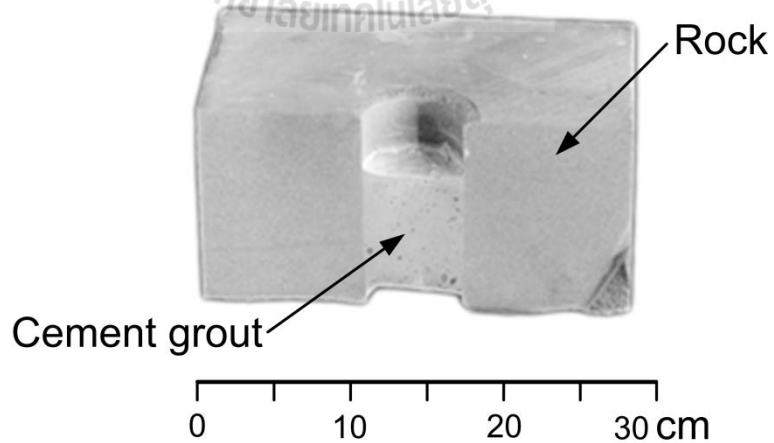
Figure 3.7 The cut away push out test specimens.

CHAPTER IV

GROUT SLURRY TESTING

4.1   Introduction

The flowability is an important parameter related to the grout mixture proportions. Good flowability or low viscosity grouts are preferred for injection purposes. The flow of grout slurry is measured by determining its viscosity and density. This chapter describes the method and results.

4.2   Test method

All grouts are prepared by mixing with the water-to-cement ratio of (w:c) 0.60. The grout preparation follows the ASTM (C938) standard practice using a Hobart type laboratory mixer.

1) The cement slurry mixtures are poured in beaker 500 ml.

2) Weighing of cement slurry mixtures in beaker and record.

3) Calculate the density of cement slurry.

4) Install the beaker of cement slurry mixtures in viscometer test machine.

5) Measure the viscosity of cement slurry mixtures and record.

The density test follows the ASTM (D854) standard practice. The viscosity test follows the ASTM (D2196) standard practice. All grout slurry test methods are shown in Figures 4.1 through 4.3
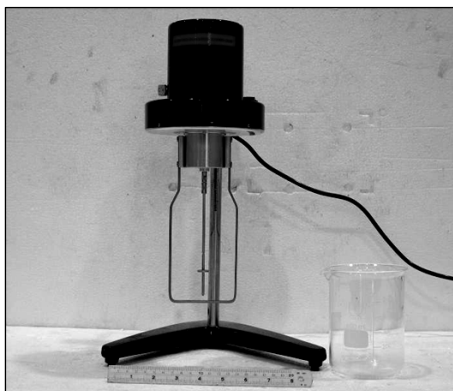
Figure 4.1 Viscometer and 500 ml beaker.

Figure 4.2 Cement slurry in beaker 500 ml.
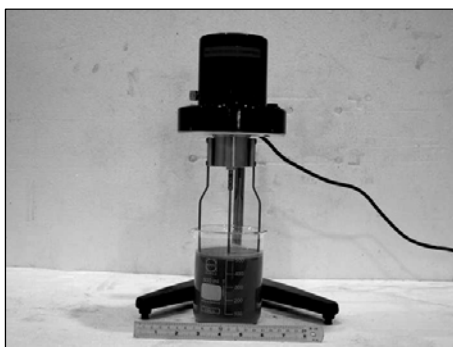
Figure 4.3 Measurement of the viscosity of cement slurry.

4.3   Test results

This section describes test results in terms of the specific gravity and viscosity. The weight of cement slurry is used to determine the density of cement slurry mixtures. The slurry viscosity are used to determine the flowability after mixed during setting time. Table 4.1 shows the results of viscosity and specific gravity measurements of the grout slurry.

Table 4.1 Properties of grout slurry for water-to-cement ratio of 0.60.

Supplier	Temperature (°Celsius)	Slurry Density (g/cc)	Specific Gravity	Dynamic Viscosity (Pa·s)
ACC	31.5	1.68	1.69	0.805
CEMEX	31.2	1.68	1.69	0.693
SCG	30.8	1.71	1.71	0.843
SCCC	31.6	1.72	1.72	0.825
TPI	31.2	1.73	1.73	0.725

The density, specific gravity, and dynamic viscosity of the slurry from all suppliers are similar. The CEMEX yields the lowest slurry viscosity of 0.693 Pa·s.

CHAPTER V

MECHANICAL TESTING OF CEMENT GROUTS

5.1   Introduction

The objective of the testing is to assess the mechanical and hydraulic performance of cement grout from 5 cement suppliers in Thailand. This chapter describes the method and results of the laboratory testing. The tests are divided into three groups; i.e. basic mechanical properties of cement grout, bond strength of cement grouts, permeability of grouting material.

5.2   Basic mechanical properties

Uniaxial, triaxial compressive strength and Brazilian tensile strength tests are performed on cement grout specimens. Their results are compared in terms of the compressive strength and elastic modulus. Strength measurements are made at 3, 7, 14, and 28 days curing time.

5.2.1   Uniaxial compressive strength tests (UCS)

Test procedure for the laboratory determination of the UCS strictly follows the American Society for Testing and Materials standard (ASTM C39) and suggested method by ISRM (International Society of Rock Mechanics) (Brown, 1981). The compressive strength of the grouts is measured from cylindrical specimens with a diameter of 54 mm and L/D = 2.5 in cylinder the grouts are cured in PVC pipe (Figure 5.1).

Strength measurements are made at 3, 7, 14, and 28 days curing. The cylindrical specimens are axially loaded at a constant rate of 0.1-0.5 MPa/second until failure. The UCS of the specimen is calculated by dividing the maximum load by the original cross-sectional area. The results of uniaxial compressive strength test are shown in Table 5.1. Figures 5.2 through 5.7 plot the uniaxial compressive strengths as a function of curing time. The average compressive strength after 28 days is 25.77±2.54 MPa. The highest compressive strengths are observed for the SCG cement supplier which equals to 27.64±2.67 MPa.
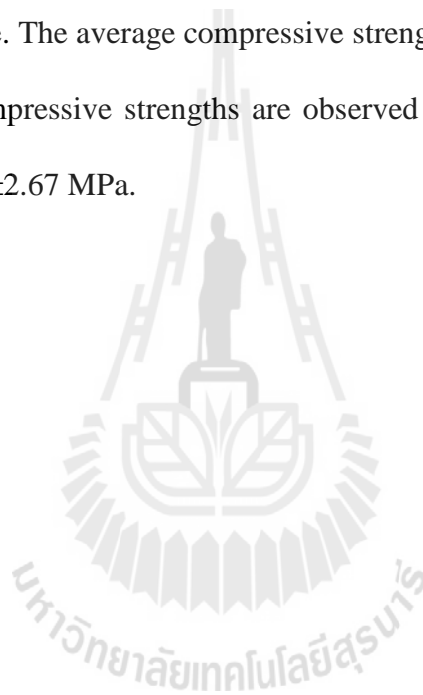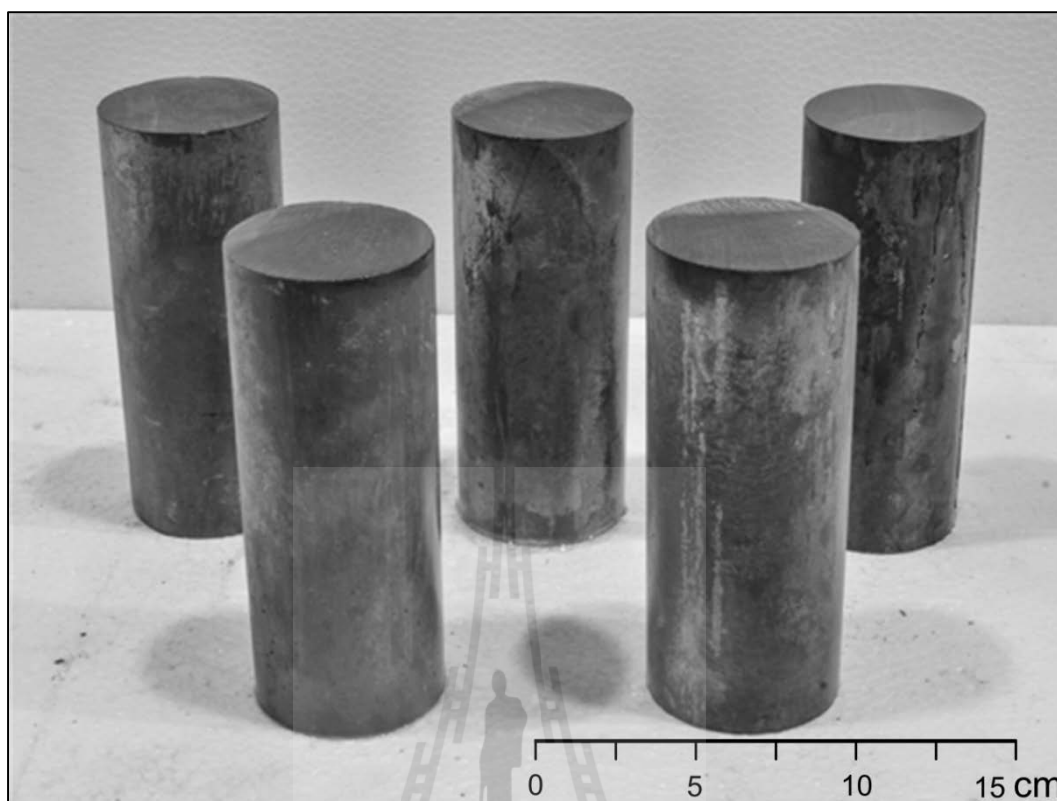
Figure 5.1 Cement grouts specimens prepared for the uniaxial compressive strength test

having 54 mm in diameter with L/D ratio of 2.5.

Table 5.1 Results of the uniaxial compressive strength testing.

Suppliers	Uniaxial Compressive Strength, σ_c (MPa)			
	3 days	7 days	14 days	28 days
ACC	09.32 ± 0.63	16.40 ± 1.59	19.72 ± 1.87	25.28 ± 2.30
CEMEX	12.38 ± 0.68	16.07 ± 1.97	20.35 ± 2.09	24.59 ± 2.60
SCG	13.82 ± 0.97	18.58 ± 1.36	22.75 ± 1.81	27.64 ± 2.67
SCCC	14.74 ± 0.95	19.05 ± 1.78	23.11 ± 2.36	25.72 ± 2.76
TPI	09.80 ± 0.78	15.92 ± 1.89	21.86 ± 2.45	25.62 ± 2.68
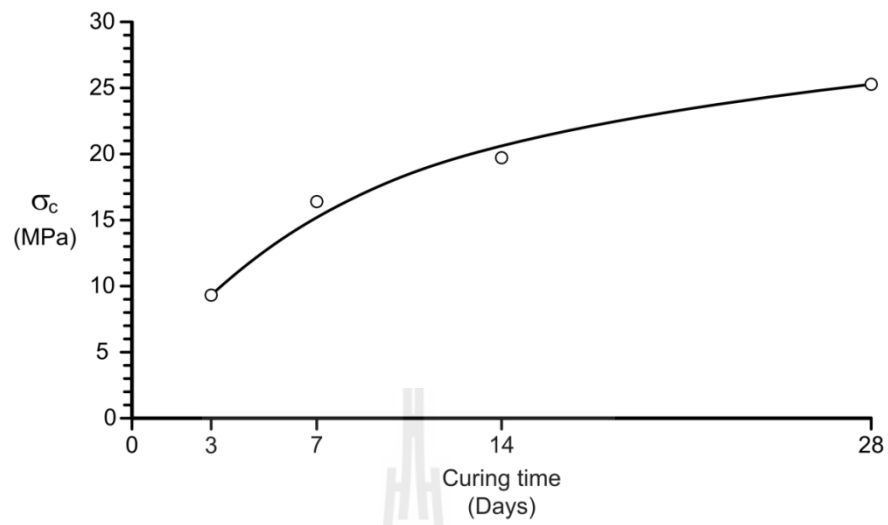
Figure 5.2 Uniaxial compressive strengths of ACC (σ_c) as a function of curing time.
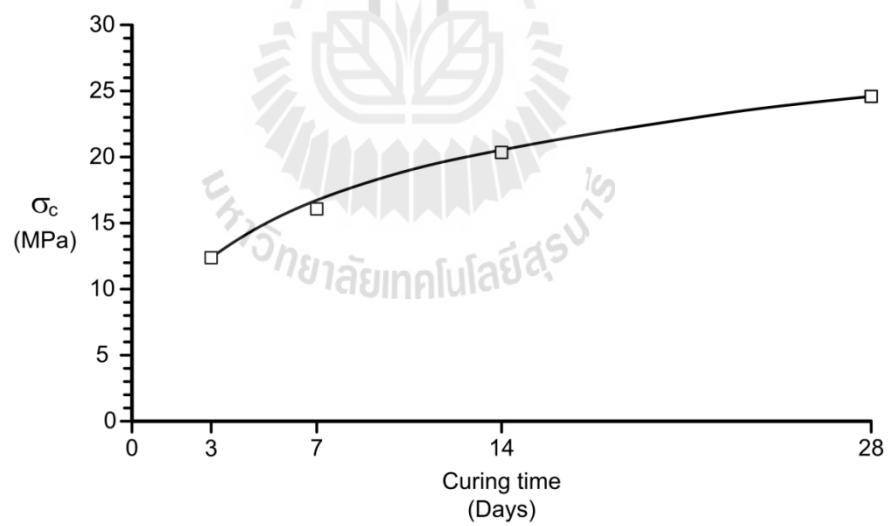
Figure 5.3 Uniaxial compressive strengths of CEMEX (σ_c) as a function of curing
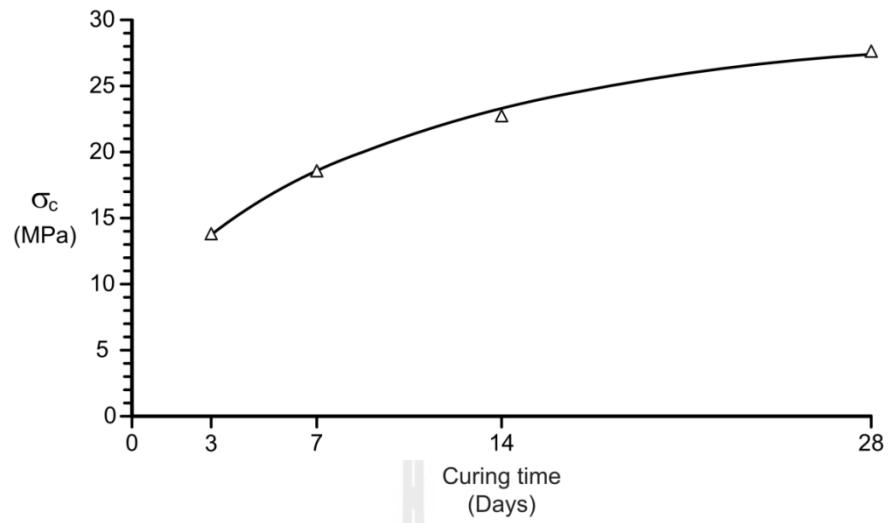
time.

Figure 5.4 Uniaxial compressive strengths of SCG (σ_c) as a function of curing time.
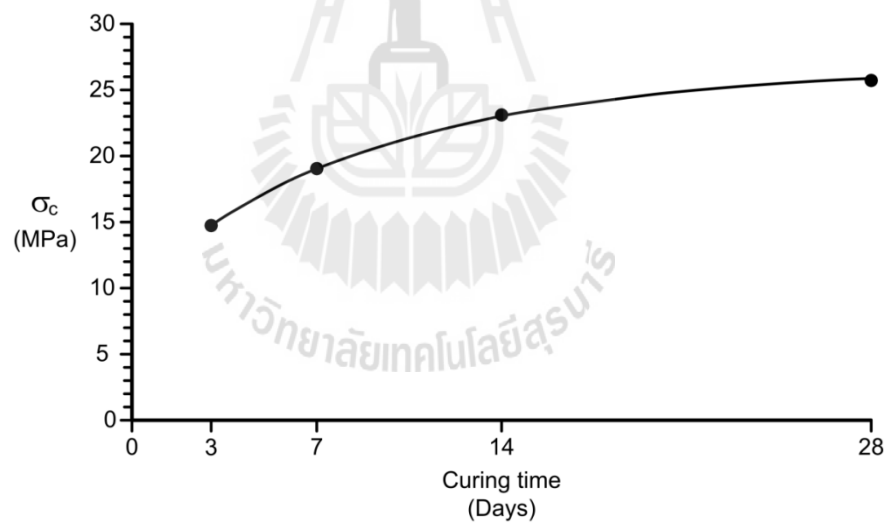
Figure 5.5 Uniaxial compressive strengths of SCCC (σ_c) as a function of curing time.
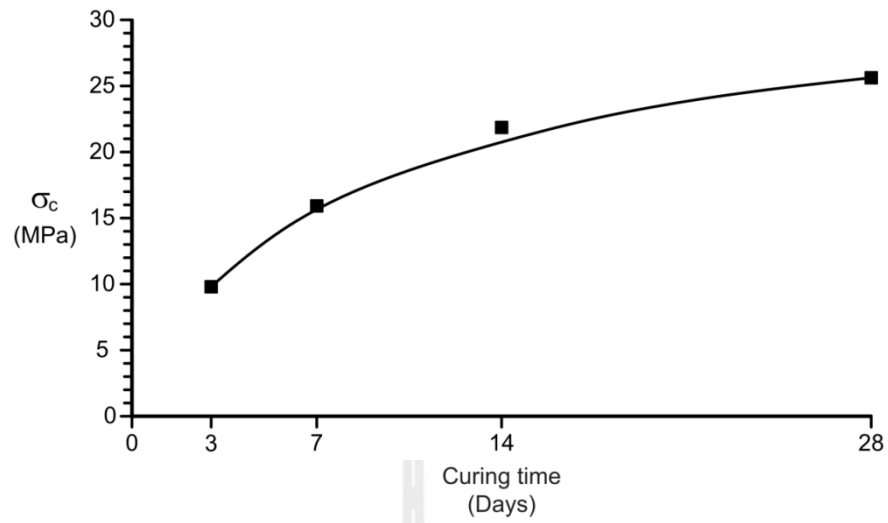
Figure 5.6 Uniaxial compressive strengths of TPI (σ_c) as a function of curing time.
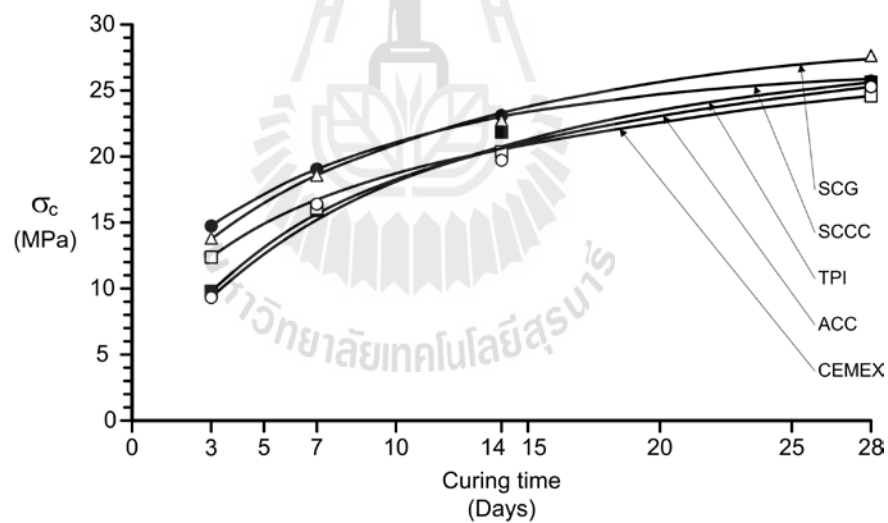
Figure 5.7 Uniaxial compressive strengths (σ_c) as a function of curing time from 5

suppliers.

5.2.2 Brazilian tensile strength tests

The objective of the Brazilian tensile strength test is to determine the indirect tensile strength of the cement grouts. The sample preparation and test procedure follow the applicable ASTM standard practice (ASTM D3967) and ISRM suggested method (Brown, 1981), as much as practical. One hundreds samples with a diameter of 54 mm are tested with L/D = 0.5. Figure 5.8 shows some specimens prepared for this test. The test is performed by increasing the axial loaded at the constant rate of 0.1-0.5 MPa/second to cement grout specimens until failure. The results of the Brazilian tensile strength test are shown in Table 5.2. Figures 5.9 through 5.14 plot the Brazilian tensile strengths as a function of curing time.
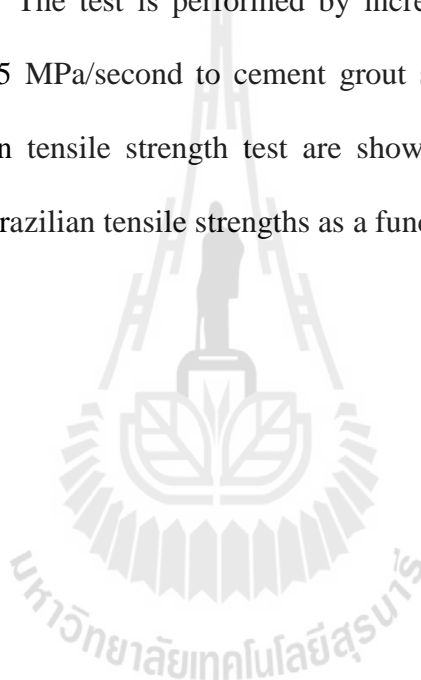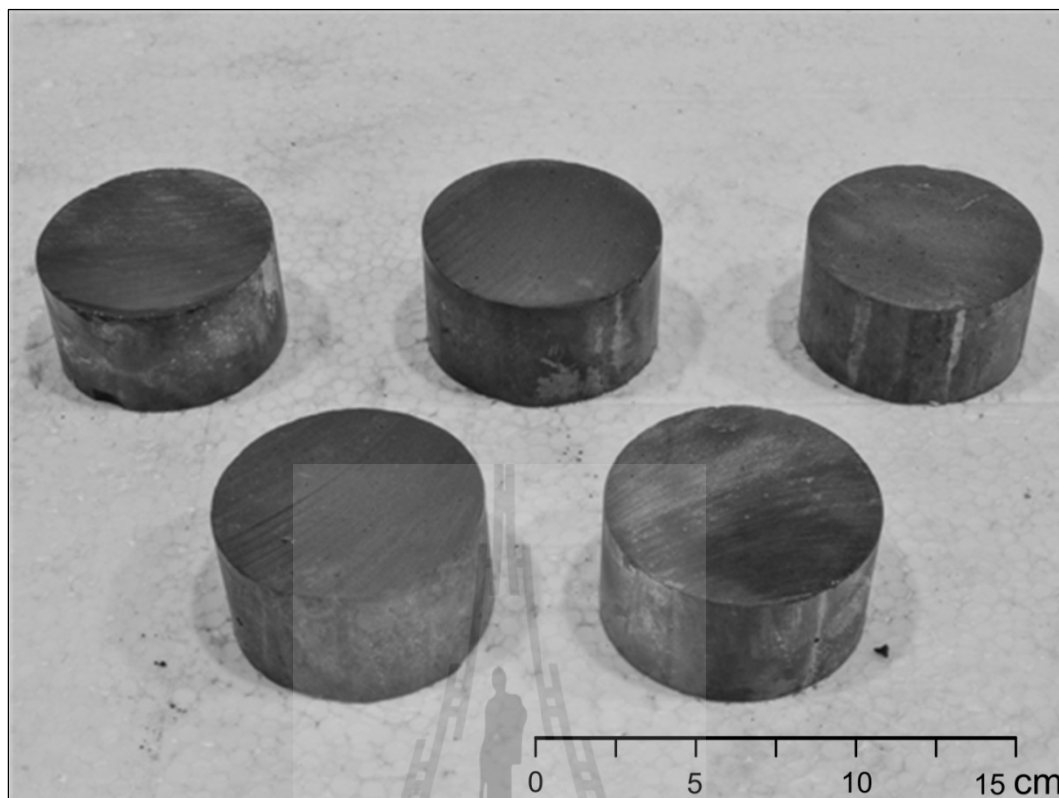
Figure 5.8 Cement grout specimens prepared for the Brazilian tensile strength test having 54 mm in diameter with L/D ratio of 0.5.

Table 5.2 Results of the Brazilian tensile strength testing.

Supplier	Brazilian tensile strength, σ_B (MPa)			
	3 days	7 days	14 days	28 days
ACC	1.40 ± 0.08	2.01 ± 0.14	2.25 ± 0.21	2.51 ± 0.32
CEMEX	2.04 ± 0.08	2.49 ± 0.16	2.78 ± 0.19	2.95 ± 0.24
SCG	1.43 ± 0.08	2.11 ± 0.15	2.44 ± 0.18	2.83 ± 0.30
SCCC	2.30 ± 0.07	2.52 ± 0.15	2.69 ± 0.19	2.87 ± 0.29
TPI	1.78 ± 0.08	2.29 ± 0.14	2.57 ± 0.19	2.80 ± 0.23
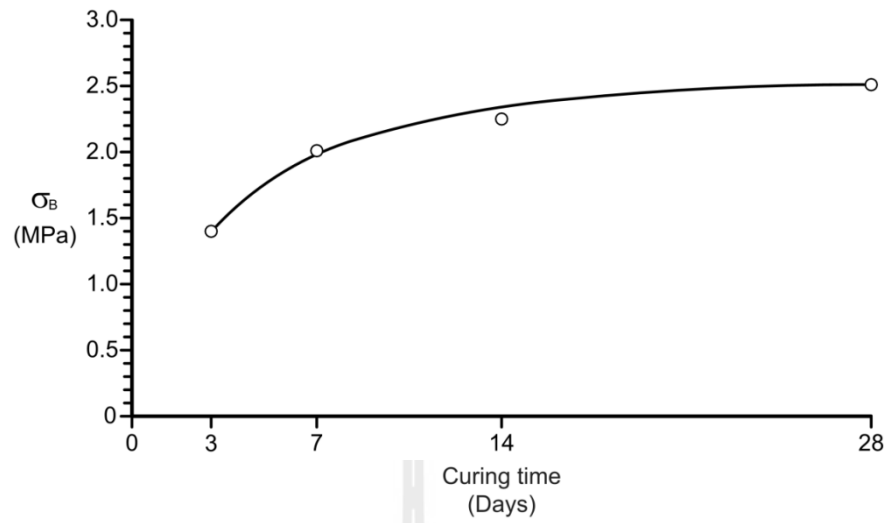
Figure 5.9 Brazilian tensile strengths of ACC (σ_B) as a function of curing time.
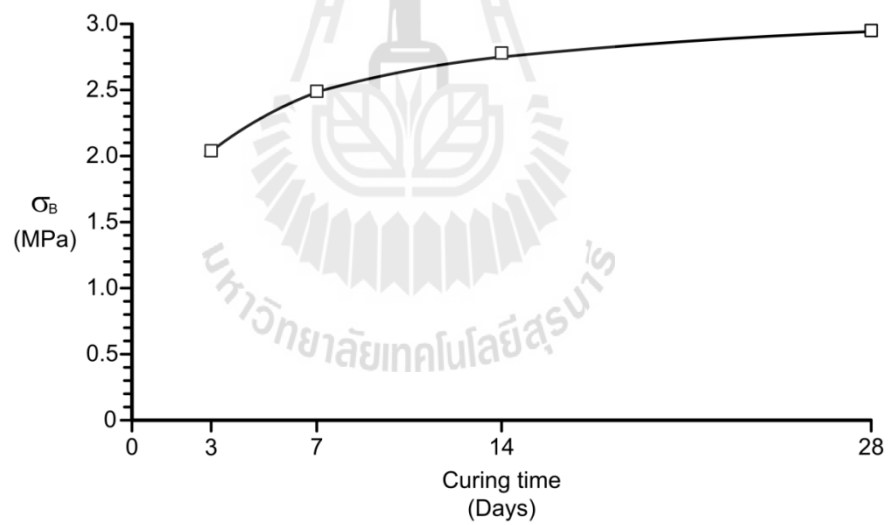

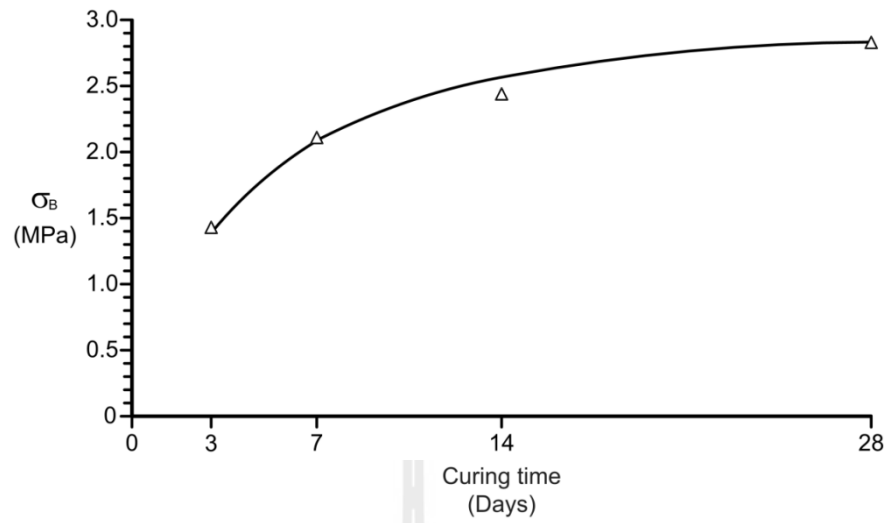**Figure 5.10** Brazilian tensile strengths of CEMEX (σ_B) as a function of curing time.

Figure 5.11 Brazilian tensile strengths of SCG (σ_B) as a function of curing time.
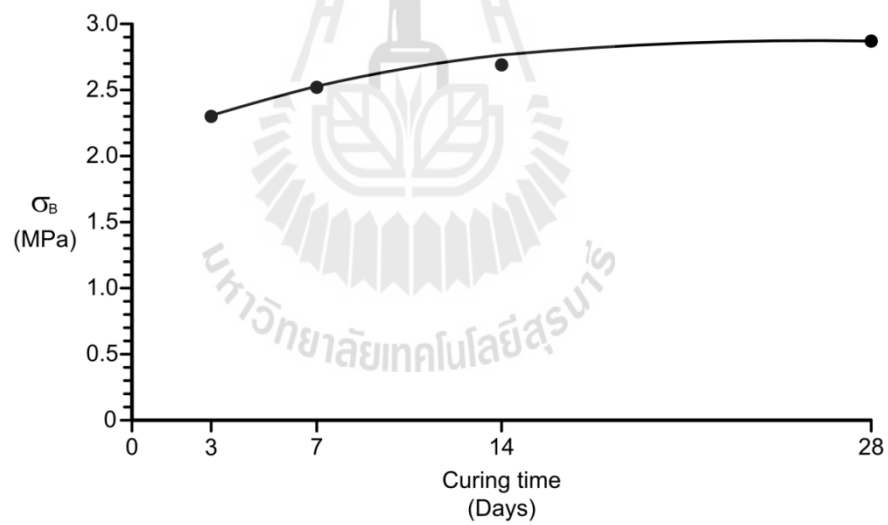

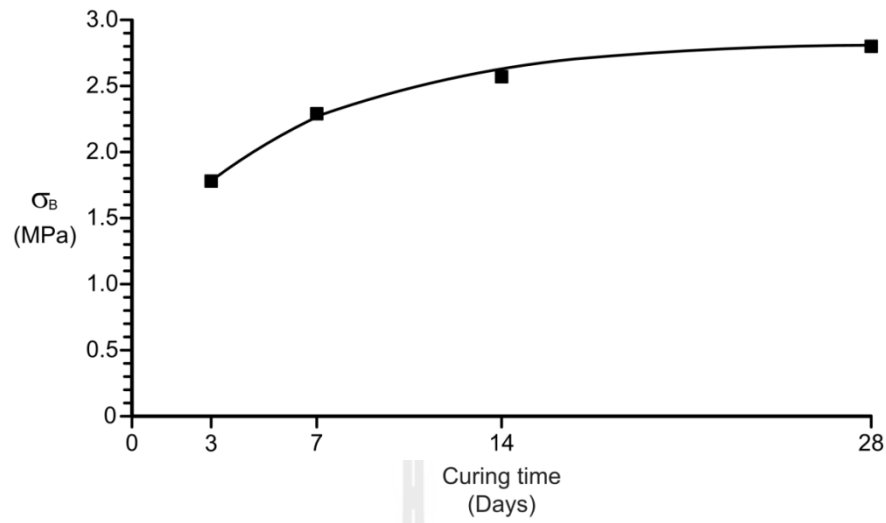**Figure 5.12** Brazilian tensile strengths of SCCC (σ_B) as a function of curing time.

Figure 5.13 Brazilian tensile strengths of SCCC (σ_B) as a function of curing time.
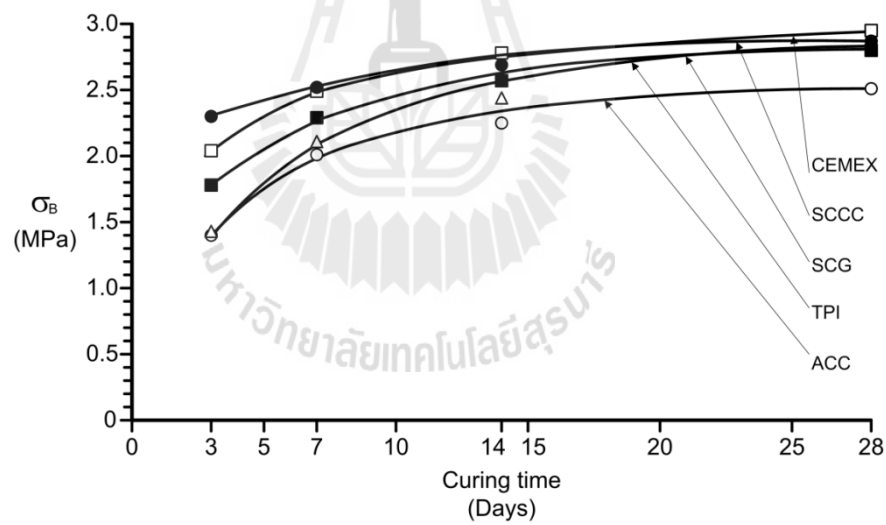

Figure 5.14 Brazilian tensile strengths (σ_B) as a function of curing time from 5

suppliers.

5.2.3 Triaxial compressive strength tests

The objective of the triaxial compressive strength test is to determine the cohesion and friction angle of the cement grouts specimens after curing for 28 days. The sample preparation and test procedure follow the applicable ASTM standard practice (ASTM D7012-04) and ISRM suggested method (Brown, 1981), as much as practical. The L/D ratio of all specimens equals 2.0 as shown in Figure 5.15. The test employs a high-pressure, high-capacity triaxial cell (Hoek Cell). The specimen is enclosed in a rubber membrane and sealed with the loading cap. The hydraulic pump is used as an ambient fluid for the application of confining pressure. In the triaxial cell pressure (minor principal stress, σ_3) is applied at 0.35, 0.70, 1.05, 1.40, and 1.75 MPa. The test is performed by increasing the axial stress (major principal stress σ_1) at a constant rate of 0.1-0.5 MPa/second until failure. The failure occurs within 5-15 minutes of loading under each confining pressure. Figure 5.16 shows the post tested specimens. The results of the triaxial compressive tests are shown in Table 5.3. Figures 5.17 through 5.21 show the Mohr circles of the results with shear stress as ordinates and normal stress as abscissas. The relationship can be represented by the Coulomb criterion :

$$\tau = c + \sigma_n \tan\phi \tag{5.1}$$

where τ is the shear stress, c is the cohesion, σ_n is the normal stress and ϕ is the internal friction angle. The average cohesion and internal friction angle after 28 days is

4.96±0.72 MPa and 42 degrees. The highest cohesion is observed for the SCG which equal to 5.42 MPa, and the highest internal friction angle are observed for the ACC which equal to 47 degrees.
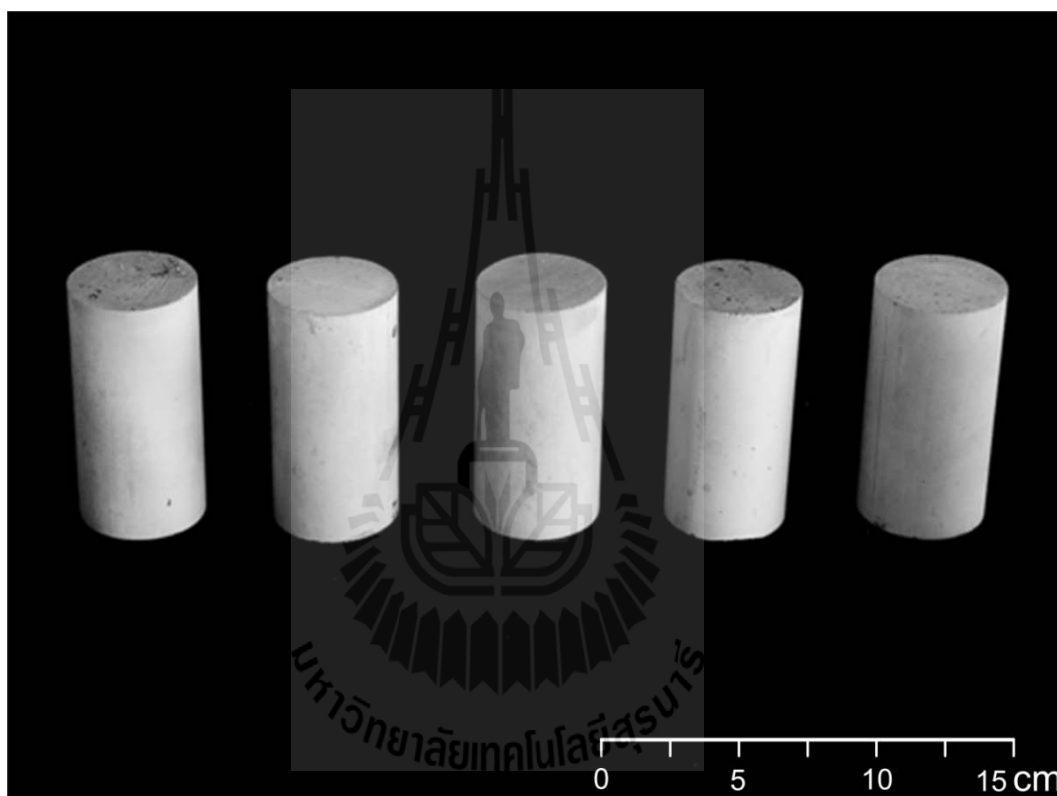

Figure 5.15 Some cement grouts specimen prepared for the triaxial compressive strength test having 54 mm in diameter with L/D ratio of 2.0.
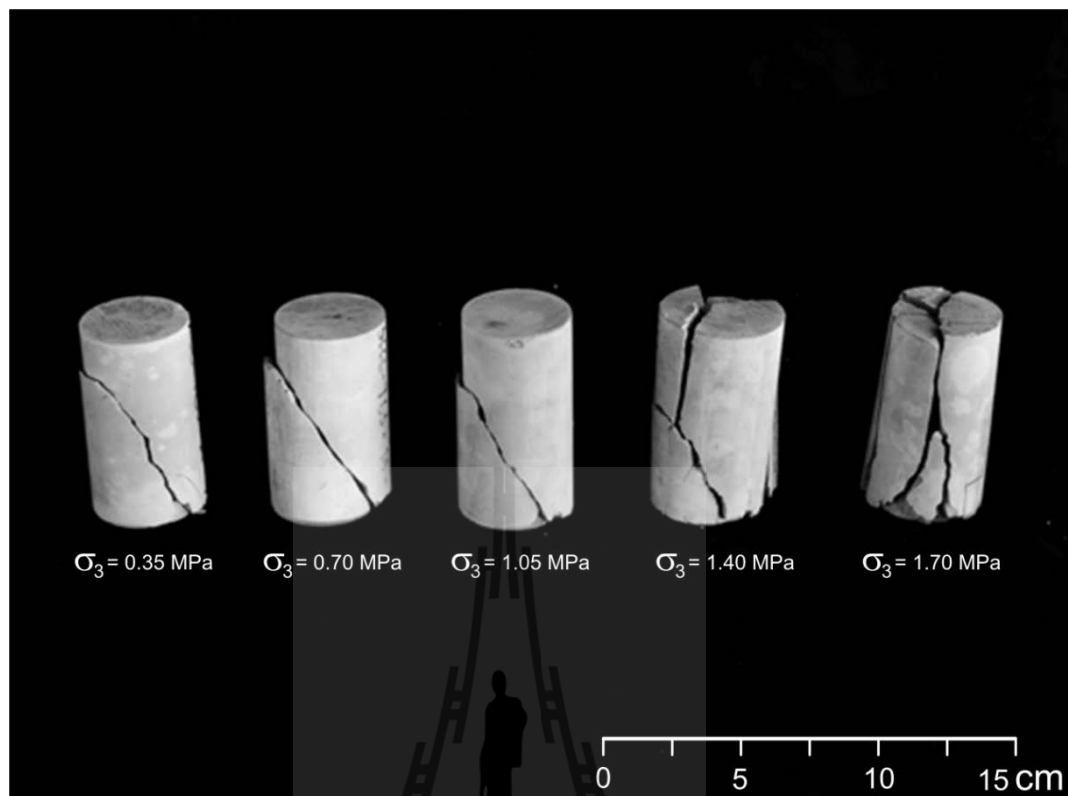
Figure 5.16 Some post-test specimens of cement grouts under various confining

pressures, σ_3 from 0.35 MPa to 1.70 MPa.

Table 5.3 Results from triaxial compression tests.

Supplier	Specimen No.	Diameter (mm)	Length (mm)	Density (g/cc)	Confining Pressure, σ_3 (MPa)	Axial Stress, σ_1 (MPa)
ACC	TCS-28-1	54.10	105.00	1.83	0.35	29.98
	TCS-28-2	53.80	107.00	1.83	0.70	31.54
	TCS-28-3	53.70	106.56	1.81	1.05	31.89
	TCS-28-4	53.34	104.12	1.82	1.40	32.44
	TCS-28-5	53.54	104.48	1.83	1.70	33.11
	Cohesion, c (MPa)				**4.96**	
	Friction Angles, ϕ (degrees)				**47**	
CEMEX	TCS-28-1	53.64	109.70	1.80	0.35	25.26
	TCS-28-2	53.62	108.98	1.81	0.70	27.66
	TCS-28-3	53.60	108.00	1.81	1.05	28.81
	TCS-28-4	53.84	109.06	1.80	1.40	29.76
	TCS-28-5	53.74	109.12	1.80	1.70	31.00
	Cohesion, c (MPa)				**5.38**	
	Friction Angles, ϕ (degrees)				**41**	
SCG	TCS-28-1	54.32	110.00	1.82	0.35	26.62
	TCS-28-2	54.00	109.62	1.81	0.70	26.97
	TCS-28-3	54.00	108.00	1.82	1.05	27.49
	TCS-28-4	53.50	110.00	1.82	1.40	28.18
	TCS-28-5	53.14	109.90	1.82	1.70	28.91
	Cohesion, c (MPa)				**5.42**	
	Friction Angles, ϕ (degrees)				**40**	

Table 5.3 Results from triaxial compression tests (continue).

| Supplier	Specimen No.	Diameter (mm)	Length (mm)	Density (g/cc)	Confining Pressure, σ_3 (MPa)	Axial Stress, σ_1 (MPa)
SCCC	TCS-28-2	54.00	111.08	1.81	0.35	28.38
	TCS-28-2	54.00	111.00	1.81	0.70	29.47
	TCS-28-3	53.90	109.38	1.82	1.05	31.77
	TCS-28-4	54.14	111.00	1.81	1.40	32.58
	TCS-28-5	54.00	110.40	1.81	1.70	33.84
	Cohesion, c (MPa)				**5.34**	
	Friction Angles, ϕ (degrees)				**44**	
TPI	TCS-28-1	54.00	108.00	1.82	0.35	25.87
	TCS-28-2	53.00	108.30	1.82	0.70	26.06
	TCS-28-3	53.00	108.00	1.83	1.05	26.2
	TCS-28-4	53.84	108.72	1.82	1.40	27.45
	TCS-28-5	53.00	108.64	1.81	1.70	29.46
	Cohesion, c (MPa)				**3.72**	
	Friction Angles, ϕ (degrees)				**40**	
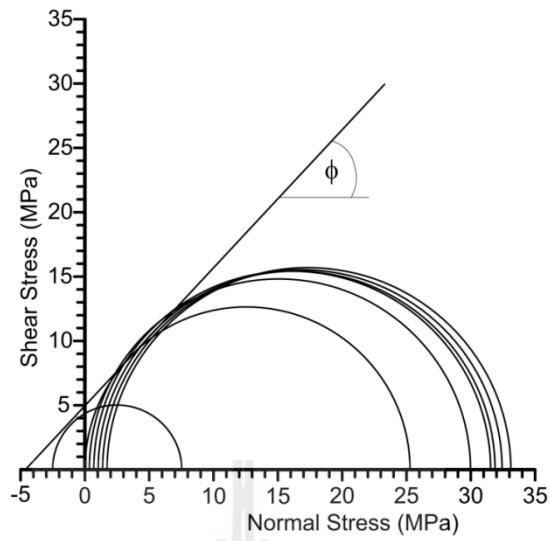
Figure 5.17 Triaxial compressive strength tests results for ACC specimens in form of

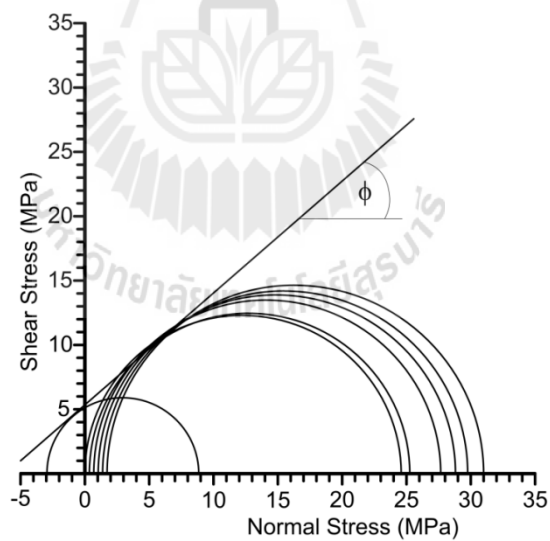Mohr's circles and Coulomb criterion.

Figure 5.18 Triaxial compressive strength tests results for CEMEX specimens in
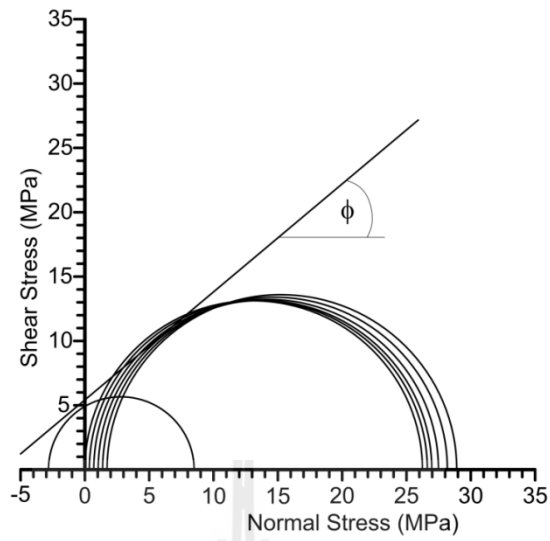
form of Mohr's circles and Coulomb criterion.

Figure 5.19 Triaxial compressive strength tests results for SCG specimens in form of
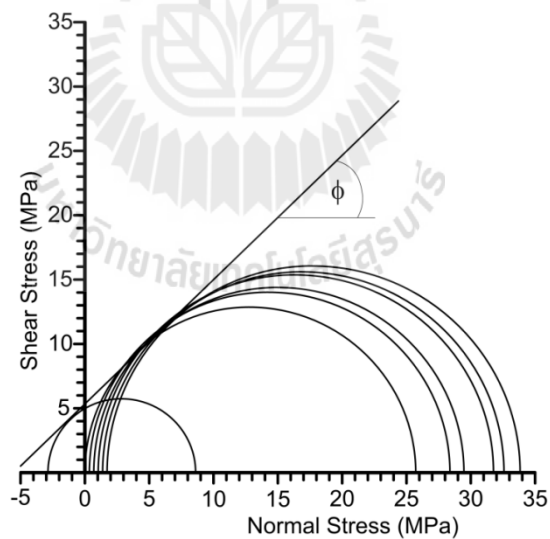
Mohr's circles and Coulomb criterion.

Figure 5.20 Triaxial compressive strength tests results for SCCC specimens in form
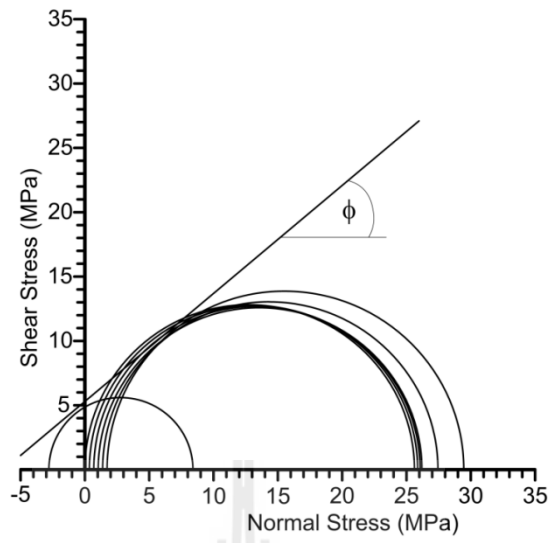
of Mohr's circles and Coulomb criterion.

Figure 5.21 Triaxial compressive strength tests results for TPI specimens in form of

Mohr's circles and Coulomb criterion.

5.3 Bond strength of cement grouts.

Two bond strength test methods are used to determine the adhesive ability of the cement grouts with rock fracture. They are the four point bending test and the push out test. Their results are compared in terms of the four point bending bond strengths and push out strengths. The measurements are investigated after 28 days of curing.

5.3.1 Four point bending test

The four point bending test determined the tensile strength of cement grout and rock fracture. The test procedure follows the ASTM (D6272) standard practice. The cement grout is casted on the tension-induced fracture of the rock cylinder with a diameter of 54 mm and length of 200 mm as shown in Figure 5.22. Five cement grouts are investigated after 28 days curing. The specimens are tested with the four point bending apparatus as shown in Figure 5.23. The bond strength of the four point bending configuration is calculated by :

$$\sigma = 16PL/3\pi D \tag{5.2}$$

where P is axial load (N); L is length of support span (m); D is diameter of specimen (m). The average bond strength after 28 days is 1.90±0.42 MPa. It is less than the average tensile strength of cement grouts. The highest bond strengths are observed for the SCCC cement supplier which equal to 2.53±0.58 MPa. Figures 5.24 through 5.28 show the post-test specimens of four point bending test.
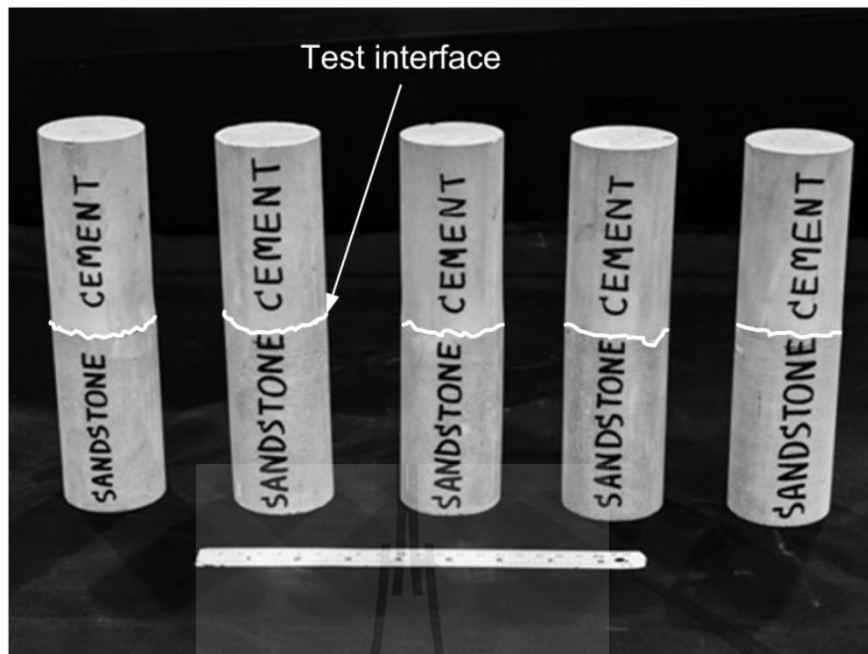
Figure 5.22 Some cement grout specimens prepared for the four point bending test having 54 mm in diameter with 200 mm length.
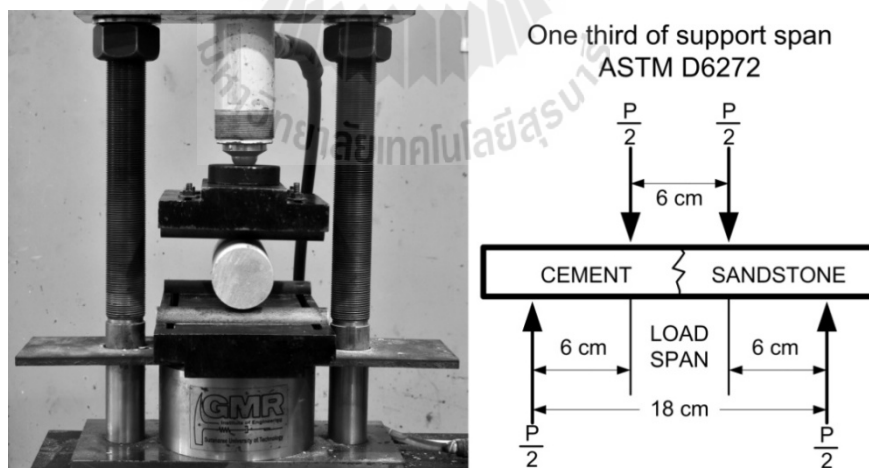

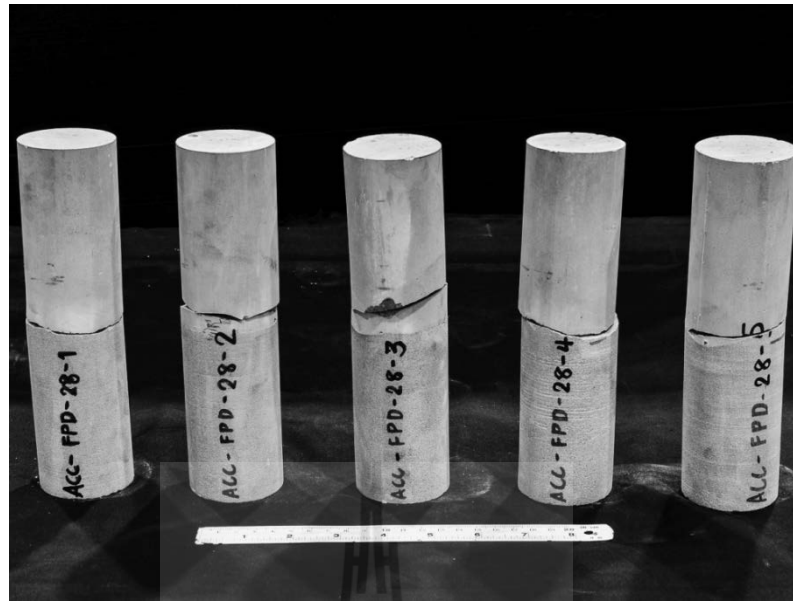**Figure 5.23** Four point bending test apparatus.

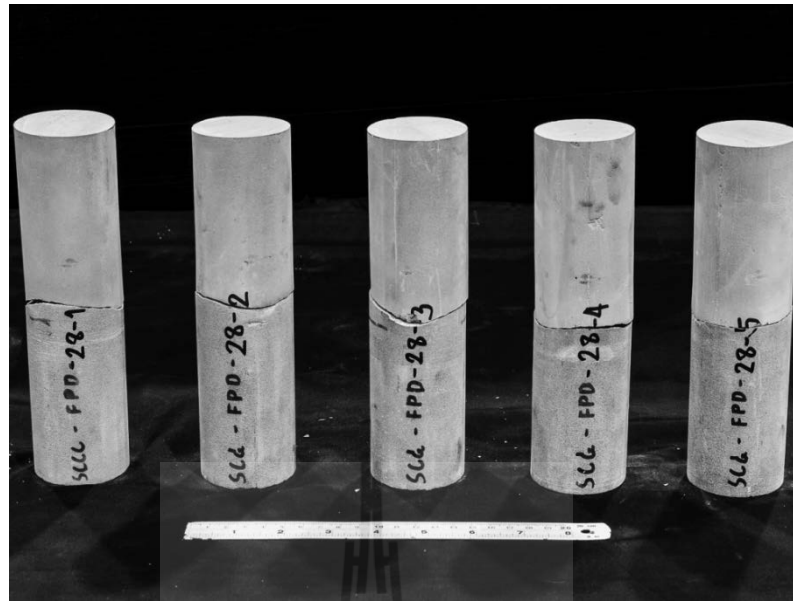**Figure 5.24** ACC post-test specimens.

Figure 5.25 CEMEX post-test specimens.

Figure 5.26 SCG post-test specimens.

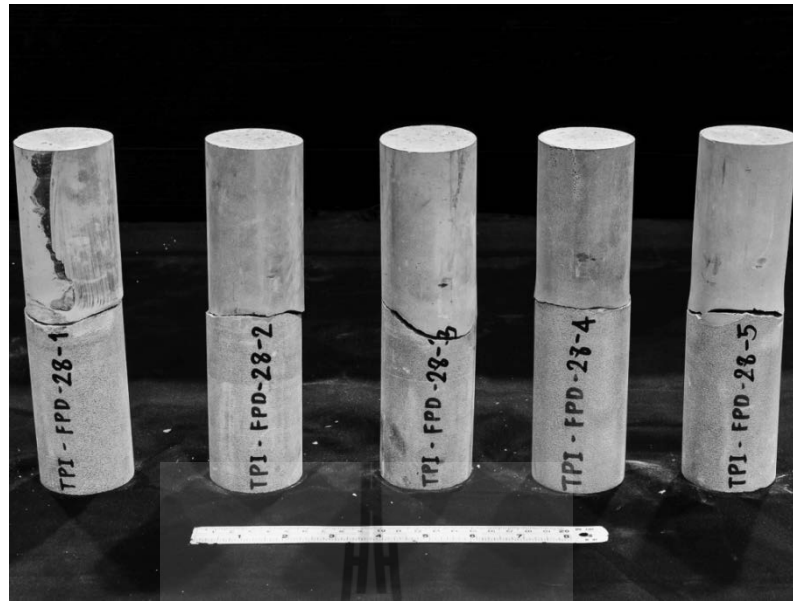**Figure 5.27** SCCC post-test specimens.

Figure 5.28 TPI post-test specimens.

5.3.1 Push out test

Push out test determines the bond strength of cement grout casted in a hole at the center of the specimen with a diameter of 35 mm and length of 70 mm. The cement grouts casted in the hole at the center of Phu Kradung sandstone are axially loaded at the constant rate of 0.1-0.5 MPa/second until sliding occurs. The strength is calculated by :

$$\sigma = P/\pi DL \tag{5.3}$$

where P is axial load (N); D is diameter of cement grout (m); L is length of cement grout (m).The average push out strength after 28 days is 4.90 MPa. It is more than the

average four points bending bond strength of cement grouts and rock fracture. The highest bond strengths are observed for the SCCC cement supplier which equals to 5.55 MPa. Figure 5.29 shows the post-test cut away specimens. Figures 5.30 through 5.34 show the shear stress as a function of shear displacement curve. Table 5.4 compares the results of four point bending bond strengths and push out strengths of cement grouts after 28 days curing.
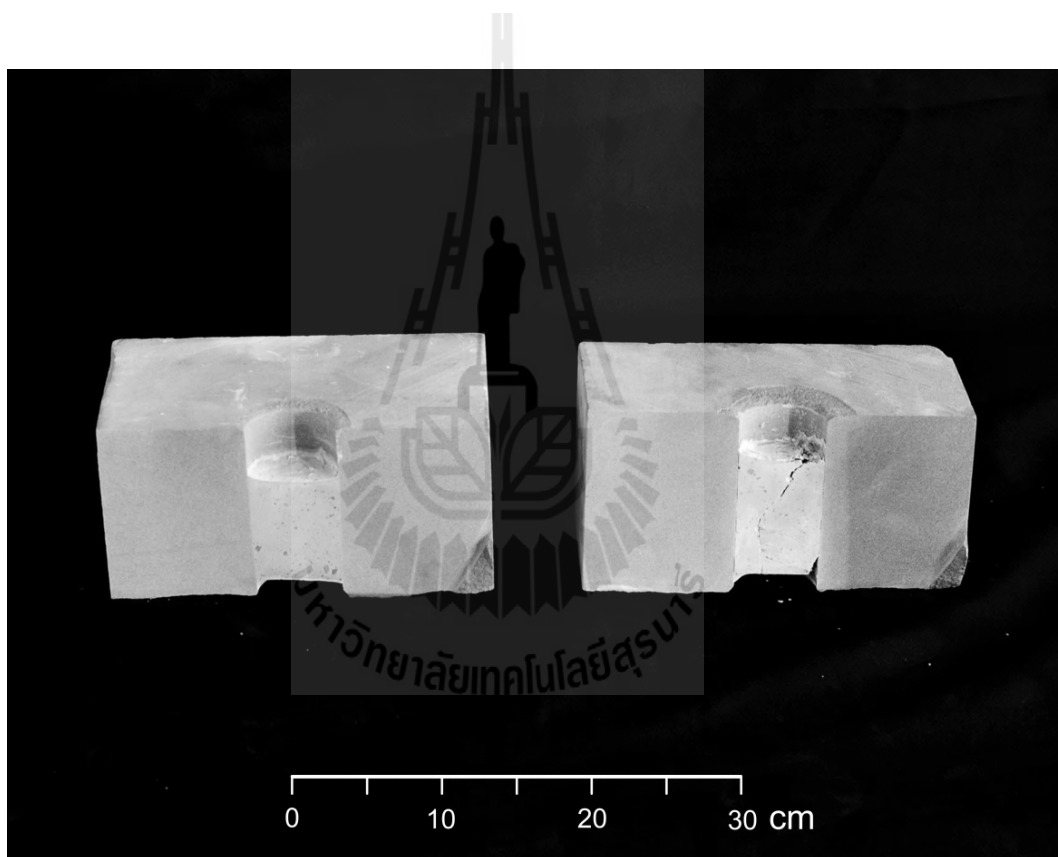

Figure 5.29 Post-test cut away specimens of push out test.
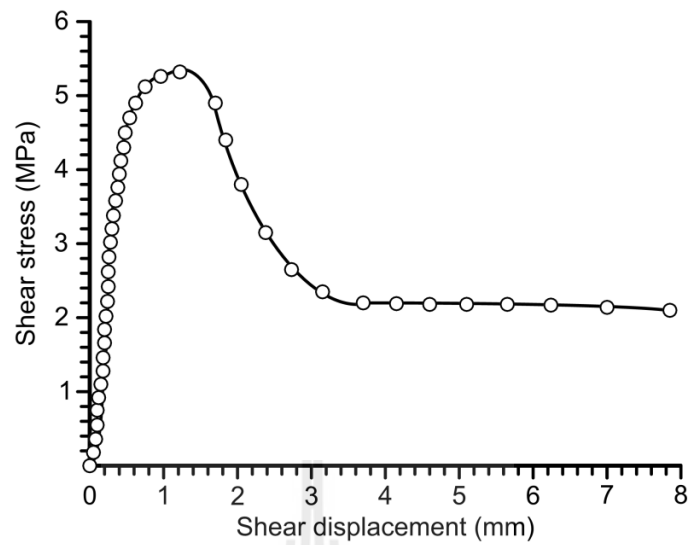
Figure 5.30 Push out tests results for ACC specimens in form of shear stress as a

function of shear displacement.

Figure 5.31 Push out tests results for CEMEX specimens in form of shear stress as a

function of shear displacement.

Figure 5.32 Push out tests results for SCG specimens in form of shear stress as a
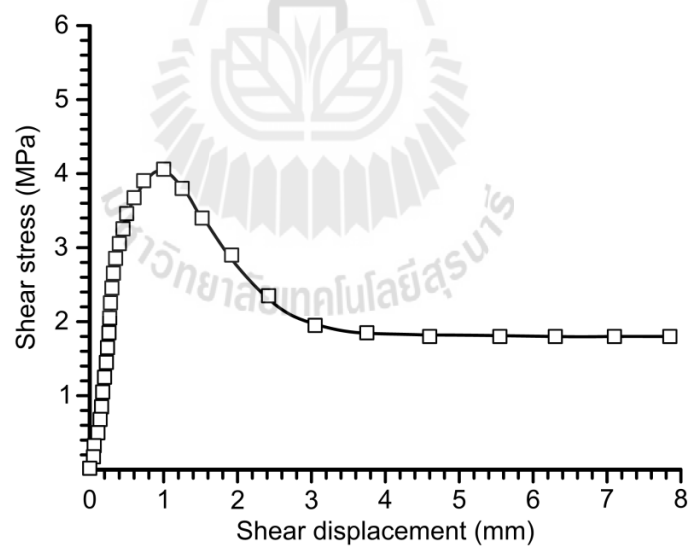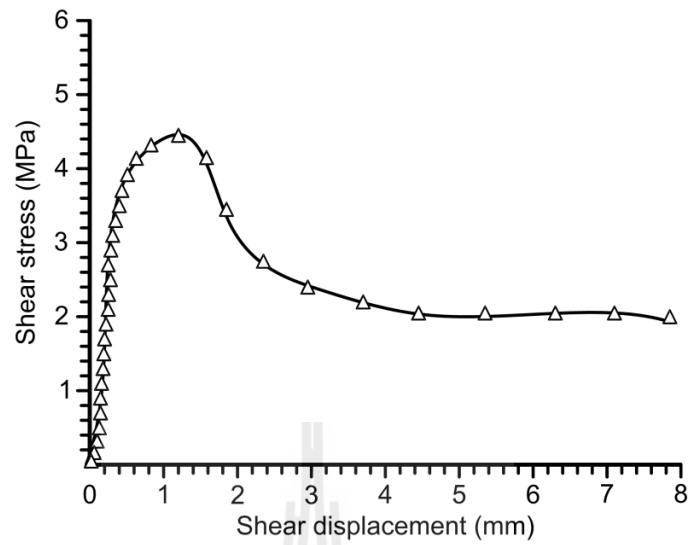
function of shear displacement.
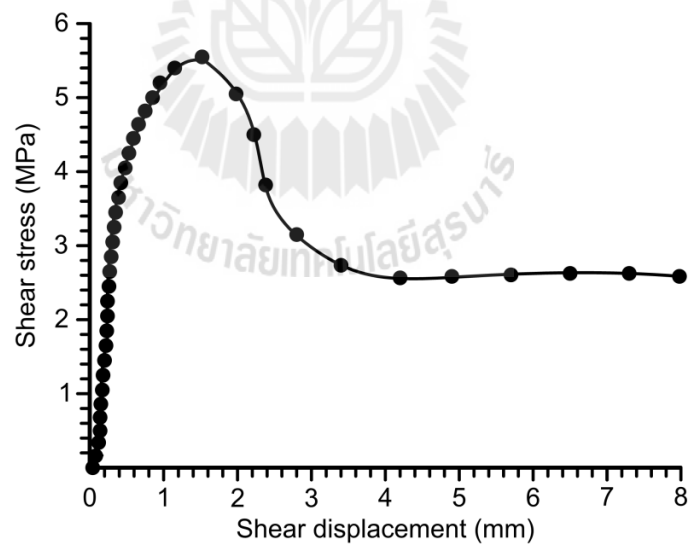
Figure 5.33 Push out tests results for SCCC specimens in form of shear stress as a

function of shear displacement.
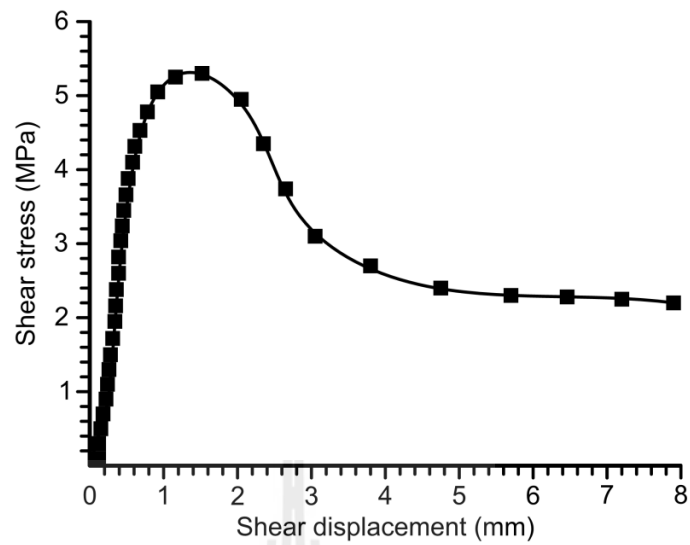
Figure 5.34 Push out tests results for TPI specimens in form of shear stress as a

function of shear displacement.

Table 5.4 Summary of results from four point bending bond strengths and push out

strengths of cement grouts after 28 days curing.

Supplier	Bond strength (MPa)	Push out strength (MPa)
ACC	1.03	5.33
CEMEX	2.46	4.06
SCG	2.07	4.45
SCCC	2.53	5.55
TPI	1.34	5.28

5.4   Permeability of grouting material.

The permeability of grouting materials is determined in terms of the intrinsic permeability (k). The constant head flow test is conducted to measure the longitudinal permeability of the grout. Test pressure and specimen configuration are measured and used to calculate the coefficient of permeability.   The permeability of the system considered herein is measured using a constant head apparatus as shown in Figure 5.34. The flow in longitudinal direction of a tested system is described by Darcy's law.   The coefficient of permeability, K, can be calculated from the equation. (Indraratna and Ranjith, 2001)

$$K = Q/Ai \tag{5.4}$$

where Q is volume flow rate (m^3/s); A is cross-sectional area of cement grout (m^2); and i is the hydraulic gradient. The intrinsic permeability (k) can be determined from the equation.

$$k = K\mu/\gamma_w \tag{5.5}$$

where K is the coefficient of permeability (m/s); μ is dynamic viscosity of liquid water from 20 degree Celsius (1.005×10^{-3} N·s/m^2); and γ_w is density of liquid water from 20 degree Celsius (9,789 N/m^3). The cylinder specimen is 10 cm in diameter and 10 cm long. After three days of curing, the specimen is carefully removed from the cast (PVC pipe), cleaned, and placed in water bath before installing in the permeability test apparatus. The permeability of the test system is measured and recorded at 3, 7, 14, and

28 days of curing periods. The results indicate that when the curing time increases the intrinsic permeability (k) of cement grout decreases. The intrinsic permeability of cement grouts as a function of curing time and shown in Figures 5.35 through 5.39.
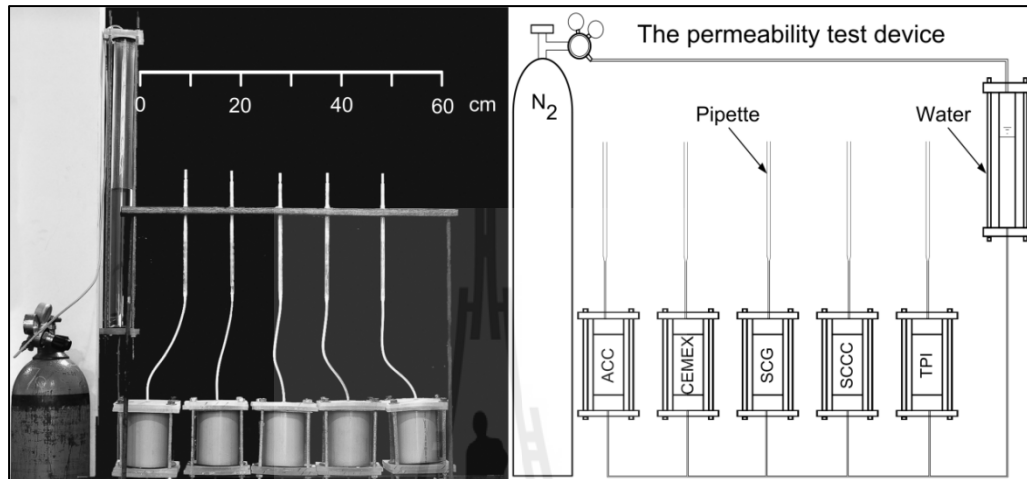
Figure 5.35 Constant head flow test apparatus used for measured the longitudinal permeability of the grout.
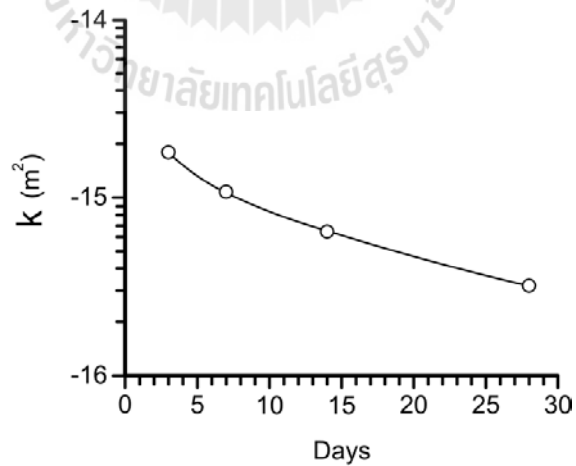
Figure 5.36 Intrinsic permeability of ACC (k) as a function of curing time
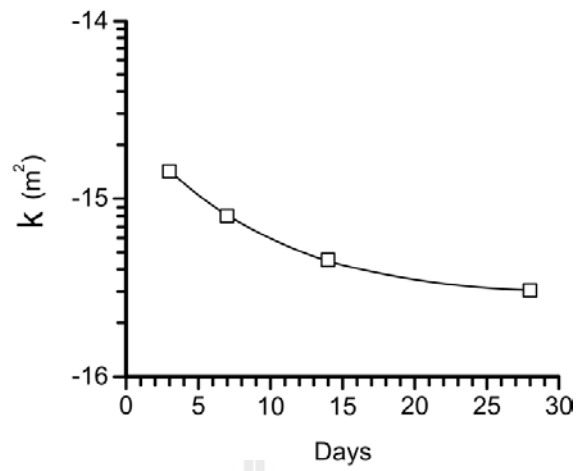
Figure 5.37 Intrinsic permeability of CEMEX (k) as a function of curing time

Figure 5.38 Intrinsic permeability of SCG (k) as a function of curing time

Figure 5.39 Intrinsic permeability SCCC (k) as a function of curing time

Figure 5.40 Intrinsic permeability TPI (k) as a function of curing time

CHAPTER VI

DISCUSSIONS AND CONCLUSIONS

6.1　Discussions and conclusions

The commercial grade cement grouts prepared from the ordinary Portland cement ASTM C150 type 1 have been tested to determine the mechanical and hydraulic performance. This study aims to determine t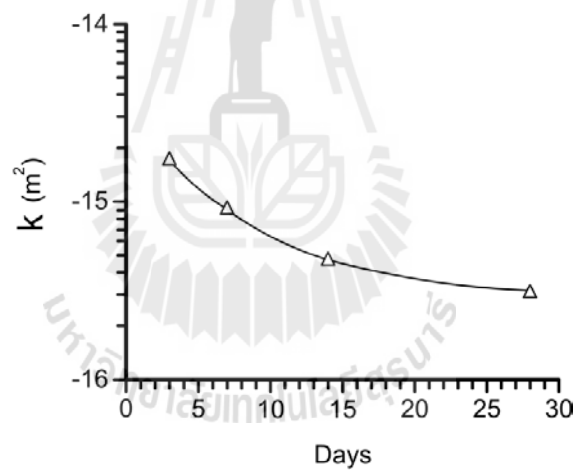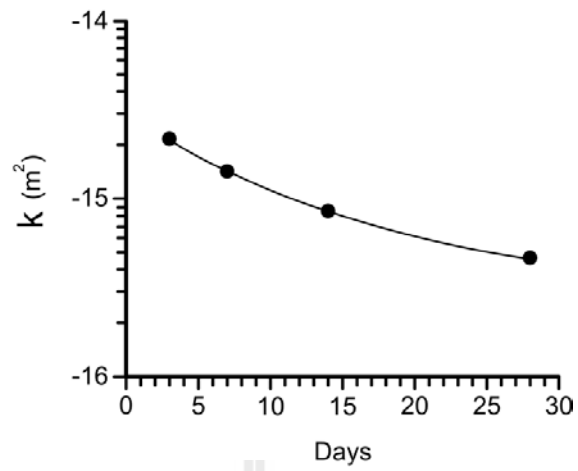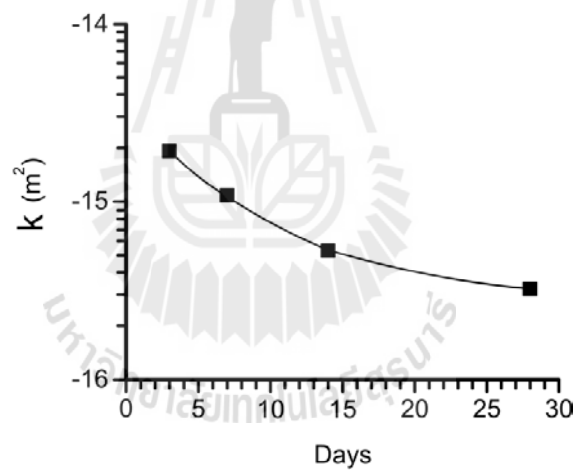he minimum slurry viscosity and appropriate strength of the grouting materials obtained from 5 cement suppliers in Thailand. The results lead to the selection of the most suitable cement supplier for grouting in rock fractures. The CEMEX yields the lowest slurry viscosity of 0.693 Pa·s. The highest compressive strengths are observed for the SCG cement supplier which equals to 27.64±2.67 MPa and elastic modulus equals to 3.86 GPa after 28 days of curing. The tensile strength and push out test in rock indicate that the bond strength between the cured grout and Phu Kradung sandstone fractures varies from 1.03 to 2.53 MPa, and the push out strength varying from 4.06 to 5.55 MPa. The permeability of the grouting materials measured from the longitudinal flow test with constant head is from 10^{-16} to 10^{-14} m^2 and decreases with curing time. The commercial grade cement grouts from CEMEX gives the lowest permeability after 28 days of curing, which equals to 3.02×10^{-16}. In summary the cement suppliers give different advantages with represent to the key properties studied has. CEMEX shows the lowest viscosity but yields the lowest compressive strength. SCG can give the highest strength and lowest permeability but its viscosity is relatively high for fracture grouting purpose. SCCC gives the highest bonding between the grout and

fracture surface. The rest of the cement suppliers show very similar mechanical and hydraulic performance.

6.2   Recommendations for future studies

The test results for the five cement suppliers are similar in terms of the strength and viscosity. To confirm the conclusions drawn in this study, more testing is required as follows.

1. Similar test should be performed on difference rock type with higher strength and larger grain size and under a variety of JRC values.

2. A relationship between the fracture roughness and fracture bond strength before and after the peak shear strengths should be determined.

3. The fracture permeability should be obtained from shearing specimen while the normal stresses should be applied at different levels.

4. The hydraulic head may be applied at different levels and probably using gas as flow medium.

REFFERENCES

ASTM Standard C150-11. 2011. Standard Specification for Portland Cement. **Annual Book of ASTM Standards**, American Society for Testing and Materials, West Conshohocken, PA.

ASTM Standard C192-07. 2007. Standard Practice for Making and Curing Concrete Test Specimens in the Laboratory. **Annual Book of ASTM Standards**, American Society for Testing and Materials, West Conshohocken, PA.

ASTM Standard C39-10. 2010. Standard Test Method for Compressive Strength of Cylindrical Concrete Specimens. **Annual Book of ASTM Standards**, American Society for Testing and Materials, West Conshohocken, PA.

ASTM Standard C938-10. 2010. Standard Practice for Proportioning Grout Mixtures for Preplaced-Aggregate Concrete. **Annual Book of ASTM Standards**, American Society for Testing and Materials, West Conshohocken, PA.

ASTM Standard D2196-10. 2010. Standard Test Methods for Rheological Properties of Non-Newtonian Materials by Rotational (Brookfield type) Viscometer. **Annual Book of ASTM Standards**, American Society for Testing and Materials, West Conshohocken, PA.

ASTM Standard D3967. Standard Test Method for Splitting Tensile Strength of Intact Rock Core Specimens. **Annual Book of ASTM Standards**, American Society for Testing and Materials, West Conshohocken, PA.

ASTM Standard D6272-10. 2010. Standard Test Method for Flexural Properties of Unreinforced and Reinforced Plastics and Electrical Insulating Materials by Four-Point Bending. **Annual Book of ASTM Standards**, American Society for Testing and Materials, West Conshohocken, PA.

ASTM Standard D7012-10. 2010. Standard Test Method for Compressive Strength and Elastic Moduli of Intact Rock Core Specimens under Varying States of Stress and Temperatures. **Annual Book of ASTM Standards**, American Society for Testing and Materials, West Conshohocken, PA.

ASTM Standard D854-10. 2010. Standard Test Methods for Specific Gravity of Soil Solids by Water Pycnometer. **Annual Book of ASTM Standards**, American Society for Testing and Materials, West Conshohocken, PA.

Akgün, H. and Daemen, J.K. (2000). Influence of degree of saturation on the borehole sealing performance of an expansive cement grout, **Cement and Concrete Research**, 30(2): 281-289.

Anagnostopoulos, C.A. 2006. Physical and Mechanical Properties of Injected Sand with Latex Superplasticized Grouts. **Geotechnical Testing Journal**. 29: 1-7.

Brown, E.T. (editor) (1981). Rock Characterization testing and monitoring: ISRM Suggested methods. The Commission on Rock Testing Methods, **International Society for Rock Mechanics**, Pergamon Press, New York, 211 pp.

Butron, C., Gustafson, G., Fransson, A., and Funehag, J. (2010). Drip sealing of tunnels in hard rock: A new concept for the design and evaluation of permeation grouting. **Tunnelling and Underground Space Technology**. 25: 114-121.

Christensen, B.J., Mason, T.O., Jennings, H.M. (1996). Comparison of measured and calculated permeability for hardened cement pastes, **Cement and Concrete Research**, 26(9): 1325-1334.

Duval, R. and Kadri, E.H. (1998). Influence of Silica Fume on the Workability and the Compressive Strength of High-Performance Concretes, **Cement and Concrete Research**, 28(4): 533-547.

Emoto, T., Thomas A., Bier. (2007). Rheological behavior as influenced by plasticizers and hydration kinetics, **Cement and Concrete Research**, 37(5): 647-654.

Fransson, A. (2001). Characterisation of a fractured rock mass for a grouting field Test. **Tunnelling and Underground Space Technology**. 16: 331-339.

Frantzis, P. and Baggott, R. (1997). Rheological characteristics of retarded magnesia phosphate cement, **Cement and Concrete Research**, 27(8): 1155-1166.

Halamickova, P. and Rachel. (1995). Water permeability and chloride ion diffusion in Portland cement mortars: Relationship to sand content and critical pore diameter, **Cement and Concrete Research**, 25(4): 790-802.

Huang, W. H. (1997). Properties of cement-fly ash grout admixed with bentonite, silica fume, or organic fiber**. Cement and Concrete Research**. 27(3): 395-406.

Huang, Z., Chen, M., Chen, X. (2003). A developed technology for wet-ground fine cement slurry with its applications, **Cement and Concrete Research**, 33(5): 729-732.

Indraratna, B., and Ranjith, P. (2001). **Hydromechanical Aspects and Unsaturated Flow in Joints Rock.** Lisse: A. A. Balkema.

Jaeger, J. C., and Cook, N. G. W. (1979). **Fundamentals of Rock Mechanics** (3rd ed.). London: Chapman & Hall.

Jarny, S., Roussel, N., Rodts, S., (2005). Rheological behavior of cement pastes from MRI velocimetry, **Cement and Concrete Research**, 35(10): 1873-1881.

Kashir, M., and Yanful, E. K. (2000). Compatibility of Slurry Wall Backfill Soils With Acid Mine Dranage. **Advances in Environmental Research** 4: 251-268.

Kim, T. K. (1998). Experimentally induced pulmonary arterial occlusion with detachable balloon in pigs: Thin-section CT findings, **Academic Radiology**, 5(12): 822-831.

Letourneur, J., Nonveiller, E. (1991), Grouting theory and practice (1989) Elsevier,Amsterdam 250., **Engineering Geology**, 31(3): 374.

Mesbah, H.A., Yahia, A., Khayat, K.H. (2011). Electrical conductivity method to assess static stability of self-consolidating concrete, **Cement and Concrete Research**, 41(5): 451-458.

Nehdi, M. (2000). Why some carbonate fillers cause rapid increases of viscosity in dispersed cement-based materials, **Cement and Concrete Research**, 30(10): 1663-1669.

Nelson, R. (1975). **Fracture Permeability in Porous Reservoirs: Experimental and Field Approach**. Ph.D. dissertation, Department of Geology, Texas A&M University.

Park, C.K., Noh, M.H., Park, T.H. (2005). Rheological properties of cementitious materials containing mineral admixtures, **Cement and Concrete Research**, 35(5): 842-849.

Schwartzentruber, L.D., Roy, R.L., Cordin, J. (2006). Rheological behavior of fresh cement pastes formulated from a Self-Compacting Concrete (SCC), **Cement and Concrete Research**, 36(7): 1203-1213.

Seidel, J.P. and Haberfield, C.M. (2002). A theoretical model for rock joints subjected to constant normal stiffness direct shear, **International Journal of Rock Mechanics and Mining Sciences**, 39(5): 539-553.

Shannag, M. J. (2002). High-performance cementitious grouts for structural repair, **Cement and Concrete Research**, 32(5): 803-808

Siqueira, C.E. and Tango. (1998). An extrapolation method for compressive strength prediction of hydraulic cement products, **Cement and Concrete Research**, 28(7): 969-983.

Valenza II, J.J., and Thomas, J.J. (2012). Permeability and elastic modulus of cement paste as a function of curing temperature, **Cement and Concrete Research**, 42(2): 440-446.

Varol, A. and Dalgıç, S. (2006). Grouting applications in the Istanbul metro, Turkey, **Tunneling and Underground Space Technology**, 21(6): 602-612.

Wong, H.S., Zimmerman, R.W., Buenfeld, N.R., (2012). Estimating the permeability of cement pastes and mortars using image analysis and effective medium theory, **Cement and Concrete Research**, 42(2): 476-483.

Yesilnacar, M.I. (2003). Grouting applications in the Sanliurfa tunnels of GAP, Turkey, **Tunnelling and Underground Space Technology**, 18(4): 321-330.

Zou, W. (1996). Synthesis and NMR assignment of two repeating units (decasaccharide) of the type III group B Streptococcus capsular polysaccharide and its 13C-labeled and N-propionyl substituted sialic acid analogues, **Carbohydrate Research**, 295: 209-228.
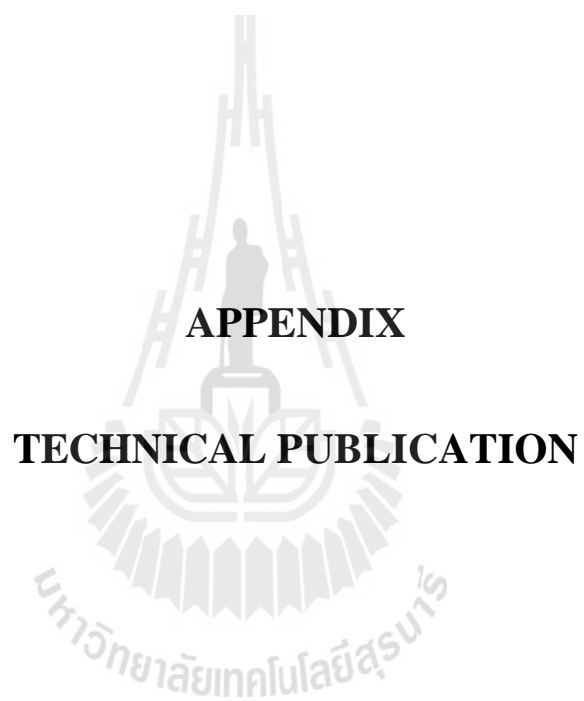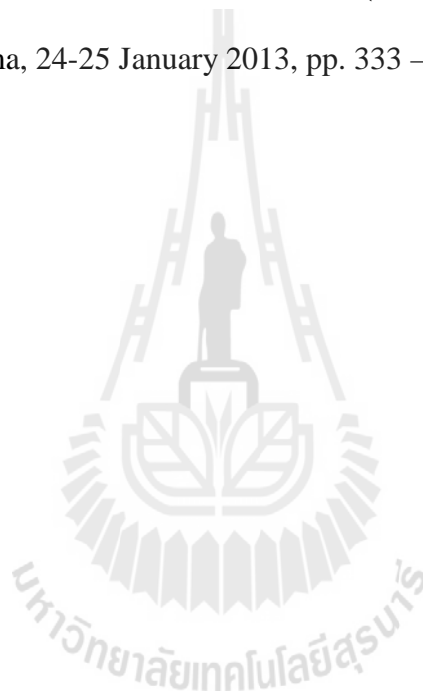
APPENDIX

TECHNICAL PUBLICATION

Technical publication

Samaiklang, W. and Fuenkajorn, K., 2013, Mechanical and hydraulic performance of cement grouts from 5 suppliers in Thailand. **In Proceedings of the Second Thailand Symposium on Rock Mechanics (ThaiRock 2013)**, Im Poo Hill Resort, Nakhonratchasima, 24-25 January 2013, pp. 333 – 342.

Mechanical and hydraulic performance of cement grouts from 5 suppliers in Thailand

W. Samaiklang & K. Fuenkajorn
Geomechanics Research Unit, Suranaree University of Technology, Thailand

Keywords: Rock fracture, bond strength, portland cement, permeability, grouting

ABSTRACT: The objective of this study is to assess the mechanical and hydraulic performance of commercial grade cement grouts in rock fracture. Their results are compared in terms of compressive strength, elastic modulus, permeability and shear strength for against rock fracture. The ordinary Portland cement (ASTM C150) type 1 from five cement supplier in Thailand has been tested. The results indicate that the viscosity of grout slurry it is 0.6 - 0.8 Pascal·sec. The compressive strength after 28 day curing times is 25.77 ± 2.54 MPa. The highest compressive strengths is from SCG cement supplier equal to 27.64 ± 2.67 MPa. The average tensile strength is 2.80 ± 0.27 MPa. The highest tensile strength is from CEMEX Thailand equal to 2.95 ± 0.10 MPa. The bond strength is 1.90 ± 0.42 MPa. The highest bond strength is from SCCC. When the curing time increases the intrinsic permeability of cement grouts decreases. Similarities and discrepancies of the grouting performance in terms of mechanical and hydraulic properties are compared to apply the commercial grade cement grouts in rock fractures.

1 INTRODUCTION

Grouting is a procedure that involves grout injection into voids, fractures, and cavities in rock mass in order to improve their strength and durability, to reduce permeability, or to reduce the deformability of the rock formations. The ordinary Portland cement (OPC) in the forms of cement-water, cement-water-sand, cement-water-additive, or cement-water-sand-additive combinations is usually used. Characteristics of the grouts are influenced by many variables. The most important one include water-cement ratio (W/C), chemical compositions, fineness of the cement, additives to the grout, speed of mixing, mixing time, efficiency of mixing, and temperature (Anagnostopoulos, 2006). This study does not attempt to evaluate these variables; rather, it is aimed at measuring relative shear strengths between cement grout and rock fracture, grout fluidity and their strength and elastic to, after curing. The cements slurry has been tested to determine the viscosity, density and flowability properties. The uniaxial compressive strength, Brazilian tensile strength, triaxial compressive strength, and the elastic modulus of the cured grouts are determined. Cylinders of the Phu Kradung sandstone are casted with the grouts for the four point bending and push out tests to determine the bond strength between the grout and rock fracture.

Mechanical and hydraulic performance of cement grouts from 5 suppliers in Thailand

2   CEMENT GROUTS

The grouting materials in this study are ordinary Portland cement ASTM (C150) type 1 obtained from five cement suppliers in Thailand, including (1) Asia Cement Public Company Limited (ACC), (2) CEMEX Thailand Cement Public Company Limited (CEMEX), (3) Siam Cement Group Public Company Limited (SCG), (4) Siam City Cement Public Company Limited (SCCC), and (5) TPI Polene Cement Public Company Limited (TPI), The chemical compositions and some physical characteristics of these materials are given in Table 1. All grouts are prepared by mixing at the water-to-cement ratio of 0.60.

The grout preparation follows the ASTM (C938) standard practice using a Hobart type laboratory mixer. The cement slurry mixtures are poured and cured in 54 mm diameter PVC pipe for the mechanical testing. The specimens are cured under distilled water at room temperature (ASTM C192) before testing.

3   ROCK SPECIMENS

The fractures in rock cylinders are artificial made by line loading in Phu Kradung sandstone blocks. These fine-grained rocks have highly uniform texture and widely expose in the north and northeast of Thailand. Samples used for the four point bending test are prepared by applying a line load at the center to induce a splitting tensile crack in 54 mm diameter, 200 mm long cylindrical specimens. The specimens for the four point bending test are shown in Figure 1. Over twenty specimens are prepared for this test. The specimen for push out test uses rectangular sandstone block with a hole drilled through the center of the specimen with a diameter of 34 mm. Figure 1 shows the specimens prepared for the push out test.

4   PROPERTIES OF GROUT SLURRY

The flowability is an important parameter related to the grout mixture proportions. The flow of grout is measured (ASTM D2196) by using a viscometer. Good flowability or low viscosity grouts is preferred for injection purposes. The flowability of the grout slurry from all suppliers are similar. The density test follows the ASTM (D854) standard practice. Table 2 shows the results of viscosity and specific gravity measurements of the grout slurry.

Table 1. Typical chemical compositions of ordinary Portland cement type I (ASTM C150).

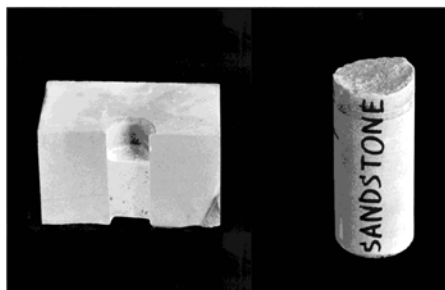| Compositions	(%)
Silicon dioxide (SiO_2)	20.9
Aluminum oxide (Al_2O_3)	5.6
Ferric oxide (Fe_2O_3)	3.1
Calcium oxide (CaO)	62.7
Magnesium oxide (MgO)	2.2
Sodium oxide (Na_2O)	0.2
Potassium oxide (K_2O)	0.8
Sulfur trioxide (SO_3)	2.9
Loss on Ignition (%)	1.3
Specific Gravity	3.15
Specific Surface (m^2/kg)	300

Figure 1. Rock specimens prepared for push out test and four point bending test.

Table 2. Properties of grout slurry for water-to-cement ratio of 0.60.

Cement supplier	Temperature (°Celsius)	Slurry Density (g/cc)	Specific Gravity	Dynamic Viscosity (Pa·s)
ACC	31.5	1.68	1.69	0.805
CEMEX	31.2	1.68	1.69	0.693
SCG	30.8	1.71	1.71	0.843
SCCC	31.6	1.72	1.72	0.825
TPI	31.2	1.73	1.73	0.725

5 BASIC MECHANICAL PROPERTIES OF GROUTS

5.1 Uniaxial Compressive Strength

The test procedure follows the ASTM (C39) and the ISRM suggested methods. The compressive strength of the grouts are measured from cylindrical specimens with a diameter of 54 mm and L/D=2.5 in cylinder that is cured in PVC pipe. Strength measurements are made at 3, 7, 14 and 28 days curing. The cement grouts are loaded at the constant rate of 0.1-0.5 MPa/second until failure. The axial displacements are monitored by displacement dial gauges. The results are reported in Table 3. Figure 2 show the average compressive strength after 28 days is 25.77 ± 2.54 MPa. The highest compressive strengths are observed for the SCG cement supplier which equals to 27.64 ± 2.67 MPa.

Table 3. Uniaxial compressive strengths of cement grouts.

Cement suppliers	Uniaxial Compressive Strength, σ_c (MPa)			
	3 days	7 days	14 days	28 days
ACC	09.32 ± 0.63	16.40 ± 0.59	19.72 ± 2.87	25.28 ± 4.30
CEMEX	12.38 ± 1.08	16.07 ± 0.97	20.35 ± 1.69	24.59 ± 2.60
SCG	13.82 ± 1.97	18.58 ± 2.36	22.75 ± 2.81	27.64 ± 2.67
SCCC	14.74 ± 0.95	19.05 ± 1.78	23.11 ± 4.96	25.72 ± 1.76
TPI	09.80 ± 1.28	15.92 ± 2.89	21.86 ± 1.45	25.62 ± 1.38

Mechanical and hydraulic performance of cement grouts from 5 suppliers in Thailand
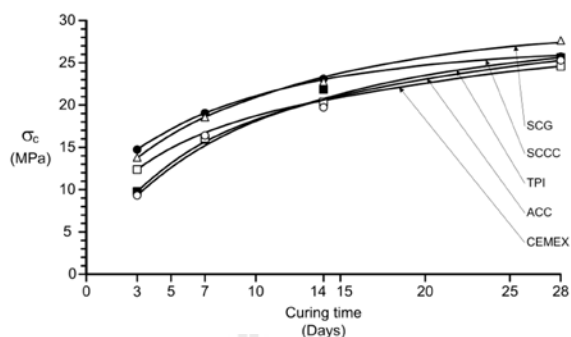

Figure 2. Uniaxial compressive strengths (σ_c) as a function of curing times.

5.2 *Brazilian Tensile Strength*

The Brazilian tension test determined the indirect tensile strength of the cement grouts. The test procedure follows the ASTM (D3967) and the ISRM suggested methods. One hundreds samples with a diameter of 54 mm are tested with L/D=0.5. The results are reported in Table 4. Figure 3 show the average tensile strength after 28 days is 2.80±0.27 MPa, it is about 10% of the compressive strength. The highest tensile strengths are observed for CEMEX Thailand cement supplier which equal to 2.95±0.10 MPa.

Table 4. Brazilian tensile strengths of cement grouts.

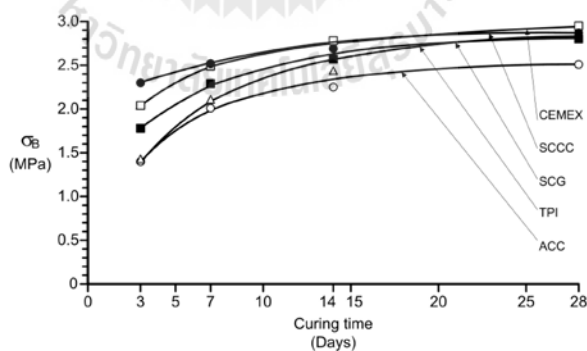| Cement supplier	Brazilian tensile strength (MPa)			
	3 days	7 days	14 days	28 days
ACC	1.40 ± 0.03	2.01 ± 0.14	2.25 ± 0.31	2.51 ± 0.22
CEMEX	2.04 ± 0.22	2.49 ± 0.29	2.78 ± 0.19	2.95 ± 0.10
SCG	1.43 ± 0.25	2.11 ± 0.09	2.44 ± 0.08	2.83 ± 0.30
SCCC	2.30 ± 0.23	2.52 ± 0.05	2.69 ± 0.29	2.87 ± 0.19
TPI	1.78 ± 0.35	2.29 ± 0.14	2.57 ± 0.19	2.80 ± 0.53

Figure 3. Brazilian tensile strengths (σ_B) as a function of curing times.

5.3 Triaxial Compressive Strength

The test procedure follows the ASTM (D7012). The triaxial compressive strength, elastic modulus, and Poisson's ratio are determined. The cement grouts specimens with a diameter of 54 mm are tested with L/D=2.0. The test employs a high-pressure, high-capacity triaxial cell (Hoek Cell). The specimen is enclosed in a rubber membrane and sealed with the loading cap. The hydraulic pump is used as an ambient fluid for the application of confining pressure. In the triaxial cell pressure (minor principal stress, σ_3) is applied at 0.35, 0.70, 1.05, 1.40 and 1.75 MPa. The test is performed by increasing the axial stress (major principal stress σ_1) at a constant rate of 0.1-0.5 MPa/second until failure. The Mohr circles and failure envelopes are applied to the results and are shown in Figure 4. These failure envelopes can be represented using Coulomb's criterion as follows,

$$\tau = c + \sigma\tan\phi \tag{1}$$

The cohesion (c) and friction angle (ϕ) for each cement supplier are shown in Figure 4.

6 BOND STRENGTH TESTING

Two bond strength test methods are used to select the adhesive ability of the cement grouts. They are the four point bending test and the push out test.

6.1 Four Point Bending Test

The four point bending test determined the bond strength of cement grout and rock fracture. The test procedure follows the ASTM (D6272). The cement grout is casted on the rough end of the rock cylinder with a diameter of 54 mm length 200 mm. Five cement grouts are investigated after 28 days curing. The specimens are tested with the four point bending apparatus as shown in Figure 5. The bond strength of the four point bending configuration is calculate in

$$\sigma = 16PL/3\pi D \tag{2}$$

where P is axial load (N); L is length of support span (m); D is diameter of specimen (m).The average bond strength after 28 days is 1.90±0.42 MPa, it less than the average tensile strength of cement grouts. The highest bond strengths are observed for the SCCC cement supplier which equal to 2.53±0.58 MPa.

6.2 Push Out Test

Push out test determined the push out strength of cement grout casted in a hole at the center of the specimen with a diameter of 35 mm and length of 70 mm. The cement grouts casted in the hole at the center of Phu Kradung sandstone are loaded at the constant rate of 0.1-0.5 MPa/second until failure. The strength is calculaded by.

$$\sigma = P/\pi DL \tag{3}$$

where P is axial load (N); D is diameter of cement grout (m) ; L is length of cement grout (m).The average push out strength after 28 days is 4.90 MPa. It more than the average four points bending bond strength of cement grouts and rock fracture. The highest push out

Mechanical and hydraulic performance of cement grouts from 5 suppliers in Thailand

strengths of the cement grouts are observed for the SCCC cement supplier which equals to 5.55 MPa. Figure 6 shows the post-test specimens. Table 5 compares the results of four point bending bond strengths and push out strengths of cement grouts after 28 days curing.
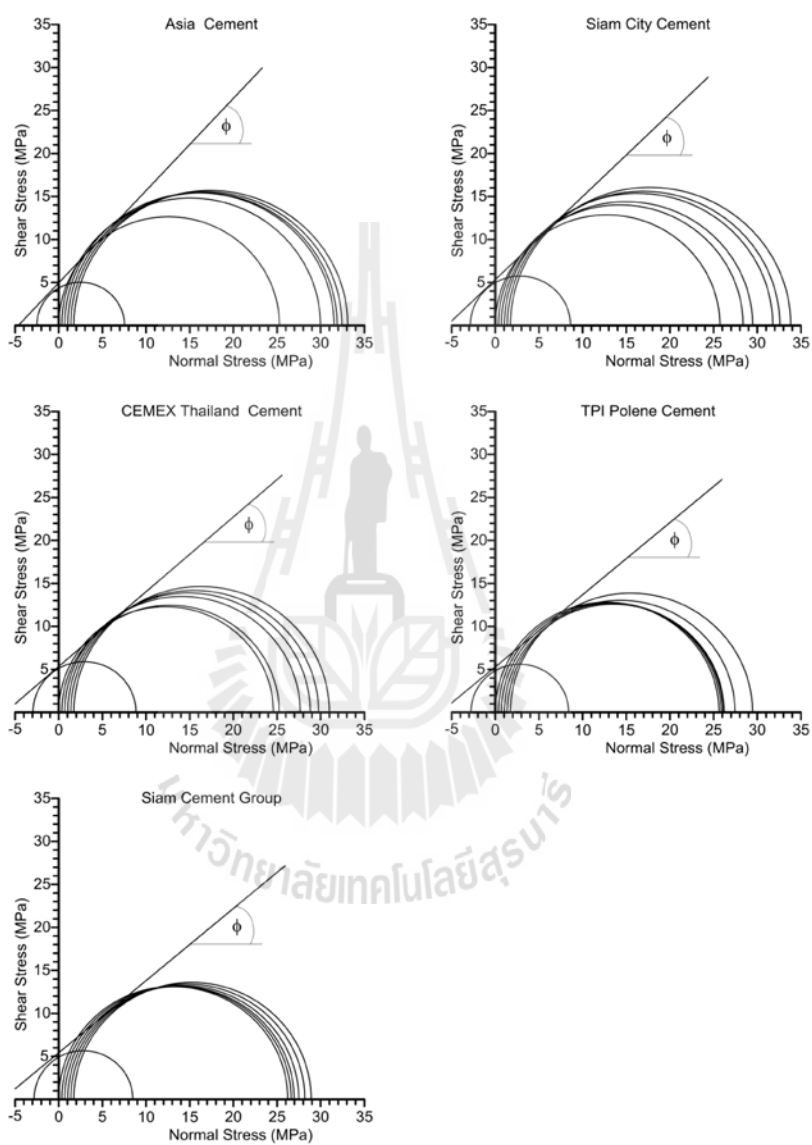

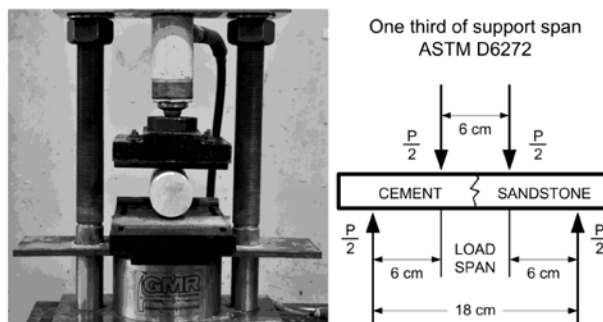Figure 4. Triaxial test results of cement grouts after 28 days curing.

338

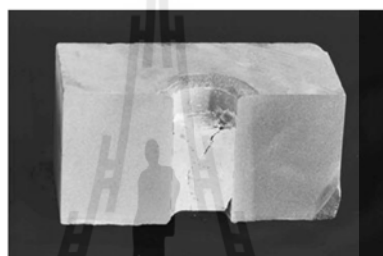Figure 5. Four point bending test apparatus.

Figure 6. Post-test specimens from push out testing.

Table 5. Four point bending bond strengths and push out strengths of cement grouts after 28 days curing.

Cement supplier	Bond strength (MPa)	Push out strength (MPa)
ACC	1.03	5.33
CEMEX	2.46	4.06
SCG	2.07	4.45
SCCC	2.53	5.55
TPI	1.34	5.28

7   PERMEABILITY OF GROUTING MATERIALS

The permeability of grouting materials is determined in term of the intrinsic permeability (k). The constant head flow test is conducted to measure the longitudinal permeability of the grout. Test pressure and specimen configuration are measured and used to calculate the coefficient of permeability. The permeability of the system considered herein is measured using a constant head apparatus as shown in Figure 7. The flow in longitudinal direction of a tested system is described by Darcy's law. The coefficient of permeability, K, can be calculated from the equation. (Indraratna & Ranjith, 2001)
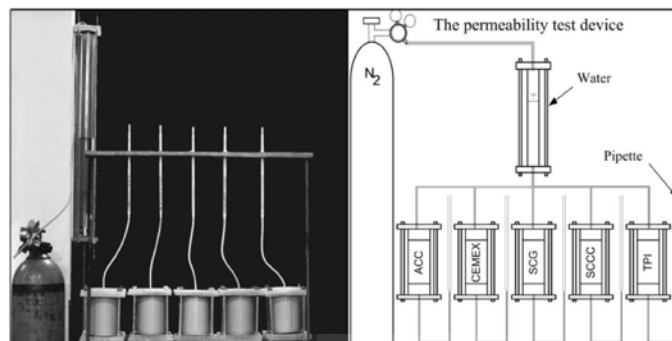
$$K = Q/Ai \qquad (4)$$

Figure 7. Constant head flow test apparatus.

where Q is volume flow rate (m^3/s); A is cross-sectional area of cement grout (m^2); and i is the hydraulic gradient. The intrinsic permeability (k) can be determined from the equation.

$$k = K\mu/\gamma_w \tag{5}$$

where K is the coefficient of permeability (m/s); μ is dynamic viscosity of liquid water from 20 degree Celsius (1.005×10^{-3} N·s/m^2); and γ_w is density of liquid water from 20 degree Celsius (9,789 N/m^3). The cylinder specimen is 10 cm in diameter and 10 cm long. After three days of curing, the specimen is carefully remove from the cast (PVC pipe), cleaned, and placed in water bath before installing in the permeability test apparatus. The permeability of the test system is measured and recorded at 3, 7, 14 and 28 days of curing periods. The results indicate that when the curing time increases the intrinsic permeability (k) of cement grout decreases. The intrinsic permeability of cement grouts as a function of curing time is shown in Figure 8.

8   DISCUSSIONS AND CONCLUSIONS

The commercial grade cement grouts tested have are ordinary Portland cement ASTM C150 type 1. This study aims to determine the minimum slurry viscosity and appropriate strength of the grouting materials. The results suggest the most suitable cement supplier for grouting in rock fractures. The CEMEX yields the lowest slurry viscosity of 0.693 Pa·s. The highest compressive strengths are observed for the SCG cement supplier which equals to 27.64±2.67 MPa and elastic modulus equals to 3.86 GPa. The bond strength test and push out test results indicate that the bond strength between the cured grout and Phu Kradung sandstone fractures is varying from 1.03 to 2.53 MPa, and the push out strength varying from 4.06 to 5.55 MPa. The permeability of the grouting materials measured from the longitudinal flow test with constant head is from 10^{-16} to 10^{-14} m^2 and decreases with curing time. The commercial grade cement grouts from CEMEX Thailand cement gives the lowest permeability after 28 days curing which equals to 3.02×10^{-16}. In summary the cement suppliers give different advantages with reported to the key properties studied have. CEMEX shows the lowest viscosity but yields the lowest compressive strength. SCG cement can give the highest strength and lowest permeability but its viscosity is relatively high for fracture grouting purpose. CEMEX give the highest bonding between the grout and fracture surface. The rest of the cement suppliers show very similar mechanical and hydraulic performance.
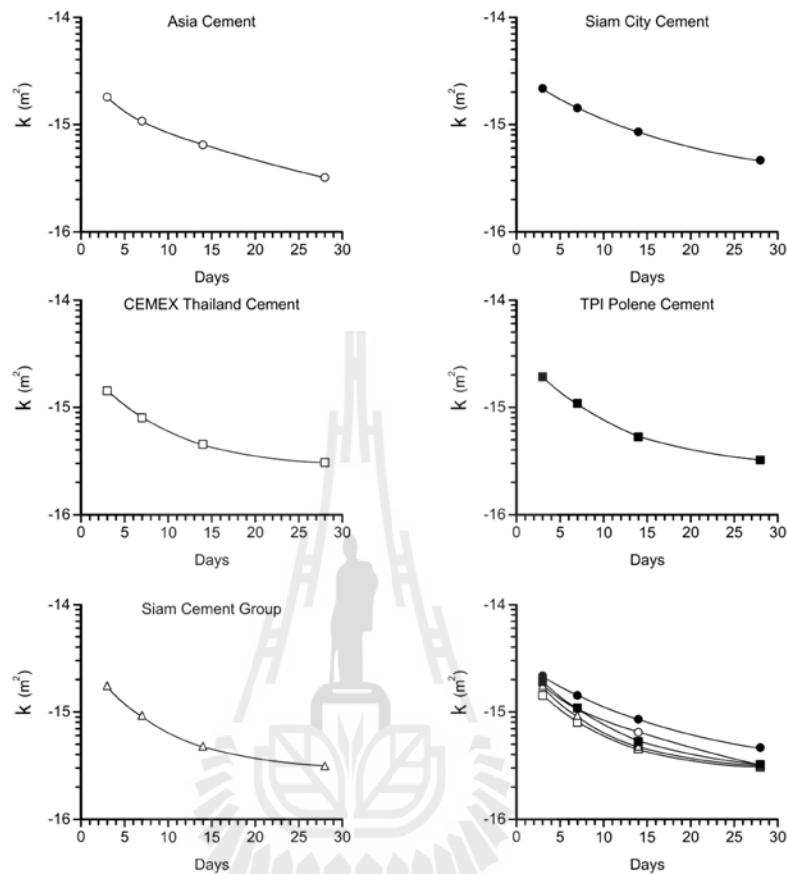
Figure 8. Intrinsic permeability (k) of cement grouts.

ACKNOWLEDGEMENT

REFERENCES

ASTM Standard C150-11. 2011. Standard Specification for Portland Cement. *Annual Book of ASTM Standards*, American Society for Testing and Materials, West Conshohocken, PA.

ASTM Standard C192-07. 2007. Standard Practice for Making and Curing Concrete Test Specimens in the Laboratory. *Annual Book of ASTM Standards*, American Society for Testing and Materials, West Conshohocken, PA.

Mechanical and hydraulic performance of cement grouts from 5 suppliers in Thailand

ASTM Standard C39-10. 2010. Standard Test Method for Compressive Strength of Cylindrical Concrete Specimens. *Annual Book of ASTM Standards*, American Society for Testing and Materials, West Conshohocken, PA.

ASTM Standard C938-10. 2010. Standard Practice for Proportioning Grout Mixtures for Preplaced-Aggregate Concrete. *Annual Book of ASTM Standards*, American Society for Testing and Materials, West Conshohocken, PA.

ASTM Standard D2196-10. 2010. Standard Test Methods for Rheological Properties of Non-Newtonian Materials by Rotational (Brookfield type) Viscometer. *Annual Book of ASTM Standards*, American Society for Testing and Materials, West Conshohocken, PA.

ASTM Standard D3967. Standard Test Method for Splitting Tensile Strength of Intact Rock Core Specimens. *Annual Book of ASTM Standards*, American Society for Testing and Materials, West Conshohocken, PA.

ASTM Standard D6272-10. 2010. Standard Test Method for Flexural Properties of Unreinforced and Reinforced Plastics and Electrical Insulating Materials by Four-Point Bending. *Annual Book of ASTM Standards*, American Society for Testing and Materials, West Conshohocken, PA.

ASTM Standard D7012-10. 2010. Standard Test Method for Compressive Strength and Elastic Moduli of Intact Rock Core Specimens under Varying States of Stress and Temperatures. *Annual Book of ASTM Standards*, American Society for Testing and Materials, West Conshohocken, PA.

ASTM Standard D854-10. 2010. Standard Test Methods for Specific Gravity of Soil Solids by Water Pycnometer. *Annual Book of ASTM Standards*, American Society for Testing and Materials, West Conshohocken, PA.

Anagnostopoulos, C.A. 2006. Physical and Mechanical Properties of Injected Sand with Latex Superplasticized Grouts. *Geotechnical Testing Journal*. 29(6): 1-7.

Indraratna, B., & Ranjith, P. 2001. *Hydromechanical Aspects and Unsaturated Flow in Joints Rock*, A. A. Balkema, Lisse.

BIOGRAPHY

Mr. Wuttichai Samaiklang was born on November 19, 1987 in Nakhon Ratchasima province, Thailand. He received his Bachelor's Degree in Engineering (Geotechnology) from Suranaree University of Technology in 2010. For his post-graduate, he continued to study for a Master's degree in the Geological Engineering Program, Institute of Engineering, Suranaree university of Technology. During graduation, 2010-2012, he was a part time worker in position of research assistant at the Geomechanics Research Unit, Institute of Engineering, Suranaree University of Technology. He published technical paper related to rock mechanics, titled Mechanical and Hydraulic Performance of Cement Grouts from 5 Suppliers in Thailand in the Proceedings of the Fourth Thailand Symposium on Rock Mechanics, Nakhon Ratchasima, Thailand.